Check for updates

AGU100 ADVANCING EARTH AND SPACE SCIENCE

JGR

Journal of Geophysical Research: Solid Earth

RESEARCH ARTICLE
10.1029/2018JB015655

Key Points:
- This paper reports on new, lightweight instrumentation to measure volcanic gases from unmanned aerial vehicles (drones)
- We measured gas ratios and gas fluxes from Turrialba and Masaya volcanoes in Central America
- Our measurements show large degassing of these two systems, reflecting their currently elevated states of unrest

Correspondence to:
J. Stix,
stix@eps.mcgill.ca

Citation:
Stix, J., de Moor, J. M., Rüdiger, J., Alan, A., Corrales, E., D'Arcy, F., et al. (2018). Using drones and miniaturized instrumentation to study degassing at Turrialba and Masaya volcanoes, Central America. *Journal of Geophysical Research: Solid Earth*, *123*, 6501–6520. https://doi.org/10.1029/2018JB015655

Received 13 FEB 2018
Accepted 1 JUL 2018
Accepted article online 5 JUL 2018
Published online 25 AUG 2018

©2018. American Geophysical Union. All Rights Reserved.

Using Drones and Miniaturized Instrumentation to Study Degassing at Turrialba and Masaya Volcanoes, Central America

John Stix[1], J. Maarten de Moor[2], Julian Rüdiger[3], Alfredo Alan[4], Ernesto Corrales[4], Fiona D'Arcy[1], Jorge Andres Diaz[4], and Marcello Liotta[5]

[1]Department of Earth and Planetary Sciences, McGill University, Montreal, Quebec, Canada, [2]Observatorio Vulcanológico y Sismológico de Costa Rica, Universidad Nacional, Heredia, Costa Rica, [3]Atmospheric Chemistry, Bayreuth Center of Ecology and Environmental Research, University of Bayreuth, Bayreuth, Germany, [4]Escuela de Física, GasLab, CICANUM, Universidad de Costa Rica, San José, Costa Rica, [5]Istituto Nazionale di Geofisica e Vulcanologia, Palermo, Italy

Abstract Gas measurements using unmanned aerial vehicles, or drones, were undertaken at Turrialba volcano, Costa Rica, and Masaya volcano, Nicaragua, in 2016 and 2017. These two volcanoes are the largest time-integrated sources of gas in the Central American Volcanic Arc, and both systems are currently extremely active with potential for sudden destabilization. We employed a series of miniaturized drone-mounted instrumentation including a mini-DOAS, two MultiGAS instruments, and an optical particle counter, supplemented by ground-based measurements. Payloads were typically 1–1.5 kg and flight times were 10–15 min. The measurements were both accurate and precise due to the inherent sensitivity of the instrumentation and the high gas concentrations, which the drones were able to sample. The quality of data obtained by our drones was comparable to that obtained by our ground-based measurements. At Turrialba in April 2017, we measured an average SO_2 flux of 1,380 ± 280 T/day, CO_2/SO_2 of 6.5, and H_2O/SO_2 of 27.8. Using these values, we calculated a CO_2 flux of 6,170 T/day and an H_2O flux of 10,790 T/day. At Masaya in May 2017, the average SO_2 flux was 1,560 ± 180 T/day, with CO_2/SO_2 of 3.9 and H_2O/SO_2 of 62.3, giving a mean CO_2 flux of 4,150 T/day and mean H_2O flux of 27,330 T/day. The elevated carbon and water fluxes and ratios are indicative of underlying magmas that are enriched in these components, resulting in the high levels of activity observed.

1. Introduction

Gas emission studies have become an integral part of volcanic monitoring approaches in the last several decades by applying various techniques for the determination of volcanic gas ratios and fluxes, such as in situ sampling (Giggenbach, 1975), remote sensing (Galle et al., 2003; Horton et al., 2006), airborne measurements in conventional aircraft (Gerlach et al., 1997; Shinohara et al., 2003; Werner et al., 2008), and in situ gas sensor instrumentation (Aiuppa et al., 2006; Shinohara, 2005). Knowledge of gas ratios and fluxes, and more importantly their changes over time and with volcanic activity, has become a useful tool to detect precursors of volcanic eruptions (e.g., Aiuppa et al., 2007; de Moor, Aiuppa, Avard, et al., 2016; de Moor, Aiuppa, Pacheco, et al., 2016).

Although remote sensing approaches allow us to observe the plume from a safe distance and therefore help to reduce risks for researchers, they still lack the ability to detect certain low-concentration gas species (e.g., HBr) and distinguish gas concentrations (e.g., H_2O) within the volcanic plume compared to the atmospheric background (Kern et al., 2017). Therefore, in situ measurements are an important source of information on volcanic gas compositions (Liotta et al., 2012; Wittmer et al., 2014).

Approaches to facilitate in situ measurements have been undertaken by using the fast developing technology of unmanned aerial vehicles (UAVs) as platforms for instrument deployments into volcanic plumes. Faivre-Pierret et al. (1980) pioneered the early use of unmanned fixed-wing aircraft by making measurements of the SO_2/HCl ratio in the plume of Mount Etna, Italy. McGonigle et al. (2008) extended this early work by using an unmanned helicopter to make gas measurements at La Fossa crater on Vulcano, Italy. They measured SO_2 fluxes by DOAS and CO_2/SO_2 ratios by MultiGAS to derive CO_2 fluxes from this volcano which was quiescently degassing. This UAV configuration allowed a ~3-kg payload, while drawbacks included the internal combustion engine of the helicopter, a heavy lead acid battery for the MultiGAS, and ground-based wind measurements from the crater rim. Shinohara (2013) used an unmanned fixed wing aircraft weighing

21699356, 2018, 8, Downloaded from https://agupubs.onlinelibrary.wiley.com/doi/10.1029/2018JB015655 by Cochrane Costa Rica, Wiley Online Library on [14/11/2025]. See the Terms and Conditions (https://onlinelibrary.wiley.com/terms-and-conditions) on Wiley Online Library for rules of use; OA articles are governed by the applicable Creative Commons License

15 kg, flight times of up to 1 hr, velocities of 100–220 km/hr, and a maximum payload of ~3 kg to conduct MultiGAS measurements in 2011 at Shinmoedake volcano, Japan, which was experiencing frequent vulcanian eruptions at the time. He observed a large temporal decrease in SO_2/H_2S which was attributed to increased degassing pressure. Mori et al. (2016) used a small octocopter with a maximum payload of ~1 kg to conduct DOAS, MultiGAS, thermal infrared, and particle measurements at Ontake volcano, Japan, after the 27 September 2014 phreatic eruption. The various measurements were made during different flights at altitudes sometimes exceeding 3,000 m. By using protective aluminum sheets to insulate the instruments from electromagnetic noise generated by the octocopter, Mori et al. (2016) were able to measure very low concentrations of gases including SO_2 at concentrations less than 1 ppm. Xi et al. (2016) measured SO_2 concentrations near Turrialba volcano, Costa Rica, by means of an unmanned aerial system tethered to balloons. They were able to use these concentrations with modeling calculations to derive SO_2 fluxes from the volcano. Diaz et al. (2015) mounted small mass spectrometers on UAV systems to measure gases at Turrialba. These studies demonstrate that previously inaccessible plume areas, either close to the vent or an elevated downwind plume, are now reachable, and the benefits for sampling and safety are obvious.

In this study we explore the feasibility of systematic plume investigations by using various UAVs and onboard instrumentation with the goal of improving volcanic gas monitoring approaches, in terms of both safety and data quality. For this work, a series of custom-made MultiGAS instruments, a miniature DOAS, a miniature particle counter, two quadcopters, and two octocopters were deployed at Turrialba and Masaya volcanoes in 2016 and 2017. In order to characterize, compare, and assess the UAV-based measurements and use the data set for gas flux estimations, traditional ground-based sampling and sensing methods were also conducted (e.g., DOAS, MultiGAS, alkaline trap sampling).

2. Instrumentation

2.1. Unmanned Aerial Vehicles

All UAV and instrumental parameters are listed in Table 1. A four-rotor multicopter with foldable arms (Black Snapper, Globe Flight, Germany; called RAVEN, Remote-controlled Aircraft for Volcanic Emission Analysis) was used during the field campaign at Masaya volcano (Rüdiger et al., 2018). It was propelled by an E800 motor set using propellers with a diameter of 13 in. and a pitch of 4.5 in. (DJI Innovations, Shenzhen, China). It was flown manually in line-of-sight conditions. The quadcopter weighed 2.3 kg including a 22.2-V (6S) 4.5-Ah battery. A maximum payload of 1.5 kg was achieved with various mounted instruments and a maximum flight time of approximately 15 min. The UAV was controlled by a NAZA M-2 flight controller (DJI Innovations, Shenzhen, China) and equipped with a datalogger (Core 2, Flytrex Aviation, Tel Aviv, Israel) with micro-SD card to record flight data from the main controller at 2 Hz, including Global Positioning System coordinates, pressure, and temperature data. The instruments were attached below and above the main body of the quadcopter with the inlets close to the center of the copter. The sampled air volume can be assumed to originate from within a radius of a few meters, which represents homogeneous conditions for a widely spread out plume.

A DJI S1000 octocopter also was used at both volcanoes (Figure 1). The drone measures 1.05 m in diameter with arms extended (folded for transport) and is 0.45 m in height. The S1000 weighs 7 kg including the battery (Tattu 22.2 V, 22 Ah, 6 cells). The maximum total takeoff weight stated by the manufacturer is ~11 kg, and we found that the S1000 could easily carry a payload of ~3 kg under field conditions. Flight times at the volcanoes were up to 15 min, at which point the battery was typically drained to less than 30%. The S1000 drone was equipped with an A3 flight controller (DJI Innovations, Shenzhen, China), allowing preprogrammed flights through DJI Ground Station Pro software. The octocopter was also fitted with a camera (GoPro X, San Mateo, USA) and video link system (Lightbridge DJI Innovations, Shenzhen, China), allowing live video streaming for manual navigation.

Typical flight times for both drones were 10–15 min. Although we operated the drones at different altitudes at the two volcanoes (2,700–3,200 m at Turrialba and 350–800 m at Masaya), we did not observe any clear differences in flight times nor was the performance of the drones significantly affected or degraded at higher elevations.

2.2. SO_2 Fluxes

The drone-mounted DOAS (DROAS) is a miniaturized ultraviolet spectroscopic system (Galle et al., 2003) designed for remote autonomous operation (Figure 2). The instrument consists of an Ocean Optics 74-DA

Table 1
UAV and Instrumental Parameters

	UAVs		
	S1000 plus	RAVEN	
Type	Octocopter	Quadcopter	
Airframe	Foldable	Foldable	
Weight	7 kg	2.3 kg	
Flight time	20 min @ 500 m a.s.l. 15 min @ 3,200 m a.s.l/w payload	15 min @ 500 m a.s.l. 8 min @ 3,200 m a.s.l/w payload	
Payload	Max. 3 kg	Max. 1.5 kg	
Flight mode	Pixhawk autopilot for programmed flight plans and manual RC/line of sight	Manual/line of sight	
	INSTRUMENTS		
Sensor	miniGAS (GLX version)	microGAS	DROAS	OPC (Alphasense)
SO_2	City Technology 3MST/F CiTiceL	City Technology 3MST/F CiTiceL	Ocean Optics USB2000+, grating#7–2,400 line holographic UV, bandwidth 281–441 nm, Options: DET2B-UV detector, L2 Lens, Slit-50	
H_2S	City Technology 3MH CiTiceL	City Technology 3MH CiTiceL		
CO_2	PP Systems SBA-5 (Analog signal)	PP Systems SBA-5		
H_2O	not installed	PP Systems SBA-5		
H_2	City Technology T3HYT	Not installed		
RH, temp, pressure	DHT 22 Sensor Module	Grant Systems Yoyo YL-RH23		
sampling rate	1 s	1 s	Typically 1 s	1.4 s
range	CO_2 0–2000 ppm, SO_2, H_2 0–200 ppm, H_2S 0–50 ppm	CO_2 0–2,000 ppm, SO_2, H_2S 0–200 ppm	281–441 nm (310−325 nm used for SO_2 retrievals)	0.3–16 μm
data logger	DRU_alpha_3 (Arduino Mega 2560 based)	Grant Systems Yoyo YL-M34	VivoStick TS10 Wifi module AW-CM25JNF; Wifi model # QCNFA425	On board
pump/flow rate (ml/min^{-1})	~1,200	~300		~220
Additional components	Adafruit Ultimate GPS MTK3339 chipset Hot Swappable 12 volt DC power module Xbee 900 MHz Telemetry Adafruit MicroSD 4 GB card Real-time visualization via Xbee USB receiver Custom software		Ocean Optics 74-DA collimating lens USGlobalSat BU-353-S4 USB GPS Receiver Voltage converter from 12 volts to 5–9 volts Castle Creations CC Bec 10A 6S switching regulator	

Note. UAV = unmanned aerial vehicle; UV = ultraviolet; GPS = Global Positioning System.

collimating lens attached to an Ocean Optics USB2000+ spectrometer powered via USB connection to a miniature onboard computer (VivoStick; Rüdiger et al., 2018). Data collection is made using MobileDOAS software (Johansson & Zhang, 2004). The instrument weighs 950 g including the 11.1 volt, 1 Ah LiPo battery and measures 18 × 11 × 6 cm. Data collection and measurement parameters are configured in MobileDOAS via wifi communication between the Vivostick computer and a laptop computer prior to drone flights. Typically, data are collected at 1 Hz, and exposure time is set according to light conditions to avoid saturation in the wavelength range of interest (310–325 nm). Data are retrieved from the VivoStick after each flight via remote desktop connection.

Conducting DROAS traverses is a flexible method for collecting high-quality spectra along optimized transects perpendicular to the plume travel direction. Flight paths are programmed in the field according to the conditions encountered, with waypoints set in the Ground Station application and then uploaded to the

21699356, 2018, 8, Downloaded from https://agupubs.onlinelibrary.wiley.com/doi/10.1029/2018JB015655 by Cochrane Costa Rica, Wiley Online Library on [14/11/2025]. See the Terms and Conditions (https://onlinelibrary.wiley.com/terms-and-conditions) on Wiley Online Library for rules of use; OA articles are governed by the applicable Creative Commons License

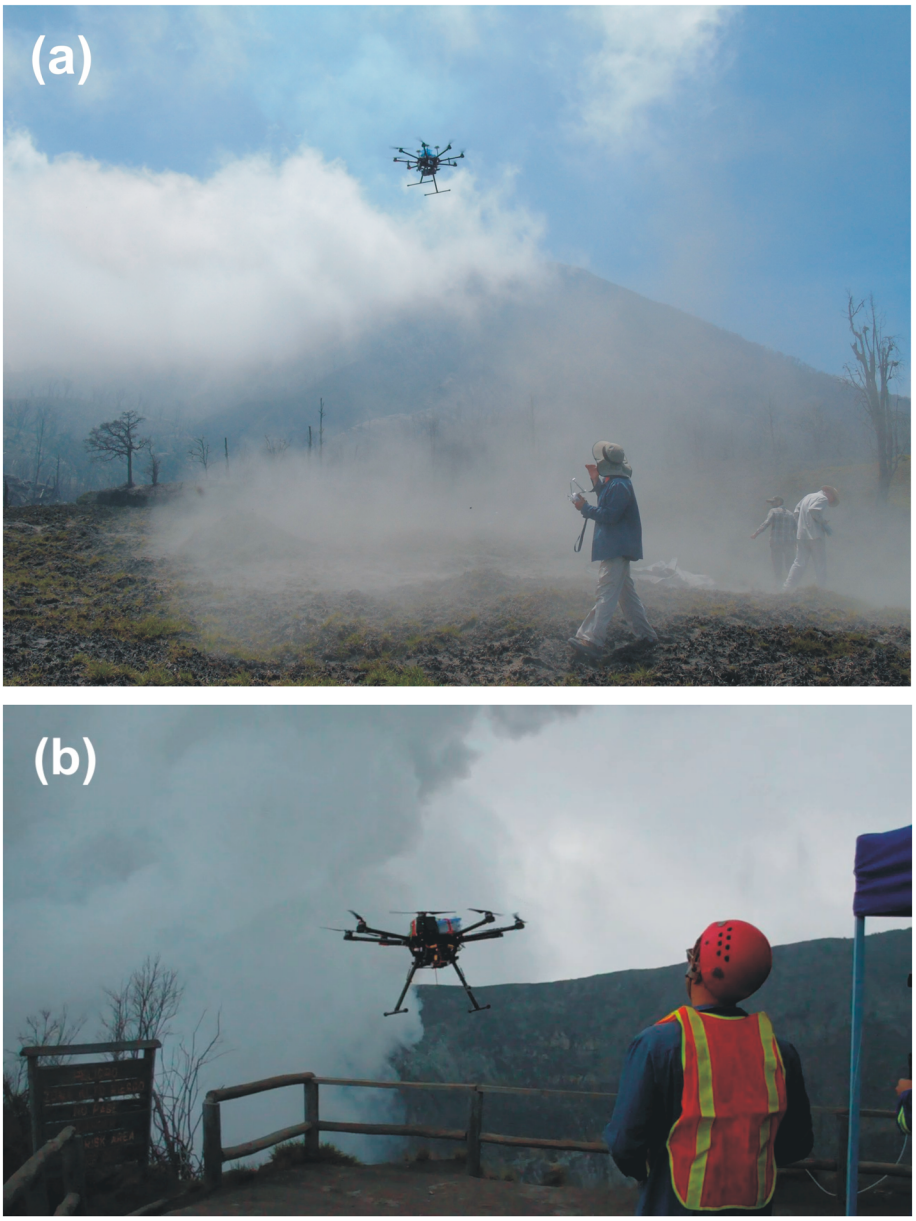

Figure 1. A DJI S1000 octocopter flying at Turrialba volcano in April 2017. (a) During takeoffs and landings, the loose volcanic ash on the ground is stirred into the air by the drone's rotors. This constitutes a potential hazard for the drone's motors and for the instrumentation. Note the white clouds and the blue-tinged volcanic gas in the background, with the 3,340-m summit of the volcano in the distance. (b) The S1000 landing at the summit mirador on 26 April 2017, with strong degassing from the summit craters evident in the background.

flight controller on the S1000 drone. The initial test flight is programmed as a long transect conducted at maximum flight speed perpendicular to estimated wind direction to identify the plume location and boundaries. Once the plume is roughly characterized in this fashion, further flights are optimized for data quality at constant flight speed and shorter flight paths, though care must always be taken to ensure that the UAV exits the plume on both ends of the traverse. Examples of flight paths are shown in Figure 3. Typically, two to four individual transects can be accomplished in a single flight, depending on drone, plume width, altitude, and wind considerations. Fast flight velocities are desirable to maximize the number of transects per flight and to record accurate snapshots of dynamic plumes. The instrument is positioned so that its telescope is pointing vertically during the flight. A constant programmed flight speed (typically 25 km/hr) results in a relatively stable drone angle (tilted in direction of travel) during the flight. We have

21699356, 2018, 8, Downloaded from https://agupubs.onlinelibrary.wiley.com/doi/10.1029/2018JB015655 by Cochrane Costa Rica, Wiley Online Library on [14/11/2025]. See the Terms and Conditions (https://onlinelibrary.wiley.com/terms-and-conditions) on Wiley Online Library for rules of use; OA articles are governed by the applicable Creative Commons License

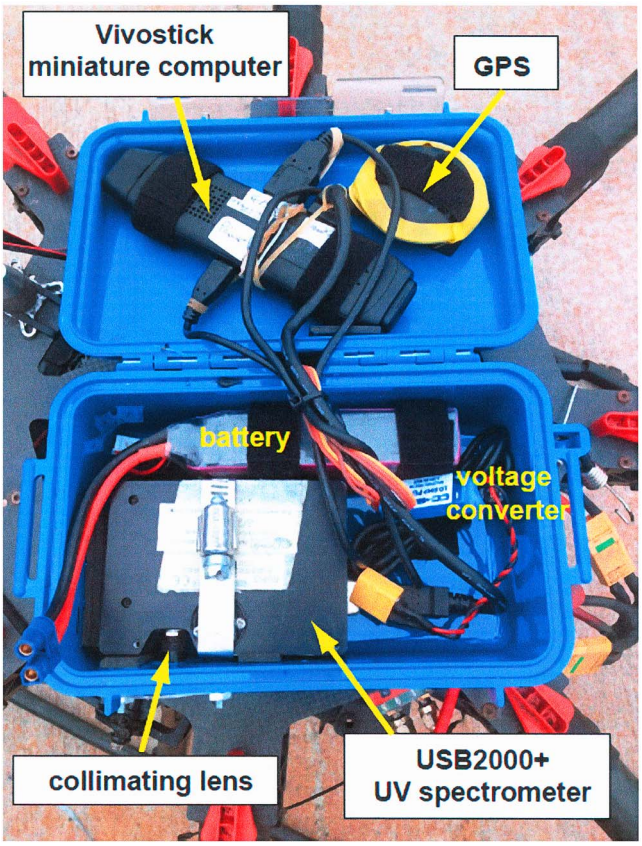

Figure 2. Details of the interior of the DROAS instrument.

found that the telescope should be angled about 15° toward the rear of the aircraft to compensate for the tilt of the S1000 drone traveling at 25 km/hr (Figure 4). Future drone-based DOAS instruments could be fitted with a gimbal to account for short-term variations in drone tilt.

2.3. CO_2, SO_2, H_2S, H_2O, and Aerosol Concentrations

We used two instrument arrays to measure CO_2, SO_2, and H_2O and their derived ratios. The first was an instrument named miniGAS, constructed at the GasLab of the Universidad de Costa Rica (Figures 5 and 6a). It consists of an arduino datalogger recording signals from an Edinburgh Gascard NG infrared spectrometer for CO_2 (concentration range: 0–3,000 ppm), and City Technology (UK) electrochemical sensors for SO_2 (0–200 ppm; 2TD2G-1A), H_2S (0–50 ppm; 2TC4E-1A), and H_2 (0–200 ppm; T3HYT). Gas is circulated through the system by a diaphragm pump at a rate of ~1,200 ml/min. The datalogger also records time, temperature, pressure, relative humidity, position, and speed via various sensors and Global Positioning System. Data are transmitted from the drone to a laptop computer via telemetry. The weight of the miniGAS is 1,500 g including battery. The second array, an instrument named microGAS, was assembled at McGill University (Figures 5 and 6b). SO_2 and H_2S are measured with CiTiceL sensors from City Technology (UK) (SO_2 0–200 ppm, 3MST/F; H_2S 0–200 ppm, 3MH). CO_2 concentrations are measured using a PP Systems SBA-5 nondispersive infrared analyzer weighing ~200 g with a range of 0–2,000 ppm and typical precision of 1–2 ppm. H_2O is measured in two ways by the microGAS: first, by a sensor incorporated into the SBA-5 CO_2 instrument, which measures absolute humidity, and second, by a separate sensor, which measures relative humidity as well as pressure and temperature (Grant Systems Yoyo YL-RH23). The gas was drawn in and circulated at a rate of ~300 ml/min by a pump in the infrared analyzer. The gas instruments are powered by a 12.8-volt, 1.5-Ah $LiFePO_4$ battery and housed in a lightweight plastic container. Particles are measured using an Alphasense OPC-N2 Optical Particle Counter based upon the principle of light scattering particles as they are transported in a sample air stream passing through a laser beam, with a sample flow rate of ~220 ml/min. The particle counter is powered by a lightweight USB 5-volt, 2.2-Ah lithium ion battery. The combined weight of the microGAS and particle counter is 1,235 g including the two batteries.

Both the miniGAS and microGAS were calibrated with standard gases in the field prior to and after flight missions. Our standard gases (Matheson TriGAS) contained 997 ppm CO_2, 350 ppm CO_2, 54 ppm SO_2, and 12 ppm H_2S, with each gas of interest in a separate tank. Each tank contained a balance of 80% N_2 and 20% O_2 thus mimicking air compositions, which is important for proper and accurate calibration of the infrared and electrochemical sensors. The certified accuracy of the standard gases is ±3%. The standard gas containing 350 ppm CO_2 was used as the zero gas for the SO_2 and H_2S calibrations.

2.4. Halogens

Due to the lack of adequate drone-based sensing or sampling methods for determination of total halogen amounts, ground-based sampling was used to investigate halogens in the plume. For this, active alkaline traps (Raschig tube, Drechsel bottle; Liotta et al., 2012; Wittmer et al., 2014) were exposed to the plume on the western rim of Santiago crater at Masaya. Based on acid–base reactions, the alkaline solution enables the quantitative collection of all acidic species in the gas and particulate phase, including CO_2, SO_2, H_2S, HCl, HF, HBr, and HI. For the Raschig tube sampling a 1-M NaOH solution was used, while the Drechsel bottle was operated with a 4-M NaOH solution (99% purity, Merck, Germany, in 18.2 MΩ water). Raschig tube sampling was performed with a GilAir Plus pump (Sensidyne, USA) for 1 hr at a flow rate of 4 L/min to determine the exact sampled air volume. Drechsel bottle samples were obtained with a custom-built pump at a flow rate of approximately 1 L/min for 18 to 30 hr. Due to the lack of datalogging with the custom pump, samples were

21699356, 2018, 8, Downloaded from https://agupubs.onlinelibrary.wiley.com/doi/10.1029/2018JB015655 by Cochrane Costa Rica, Wiley Online Library on [14/11/2025]. See the Terms and Conditions (https://onlinelibrary.wiley.com/terms-and-conditions) on Wiley Online Library for rules of use; OA articles are governed by the applicable Creative Commons License

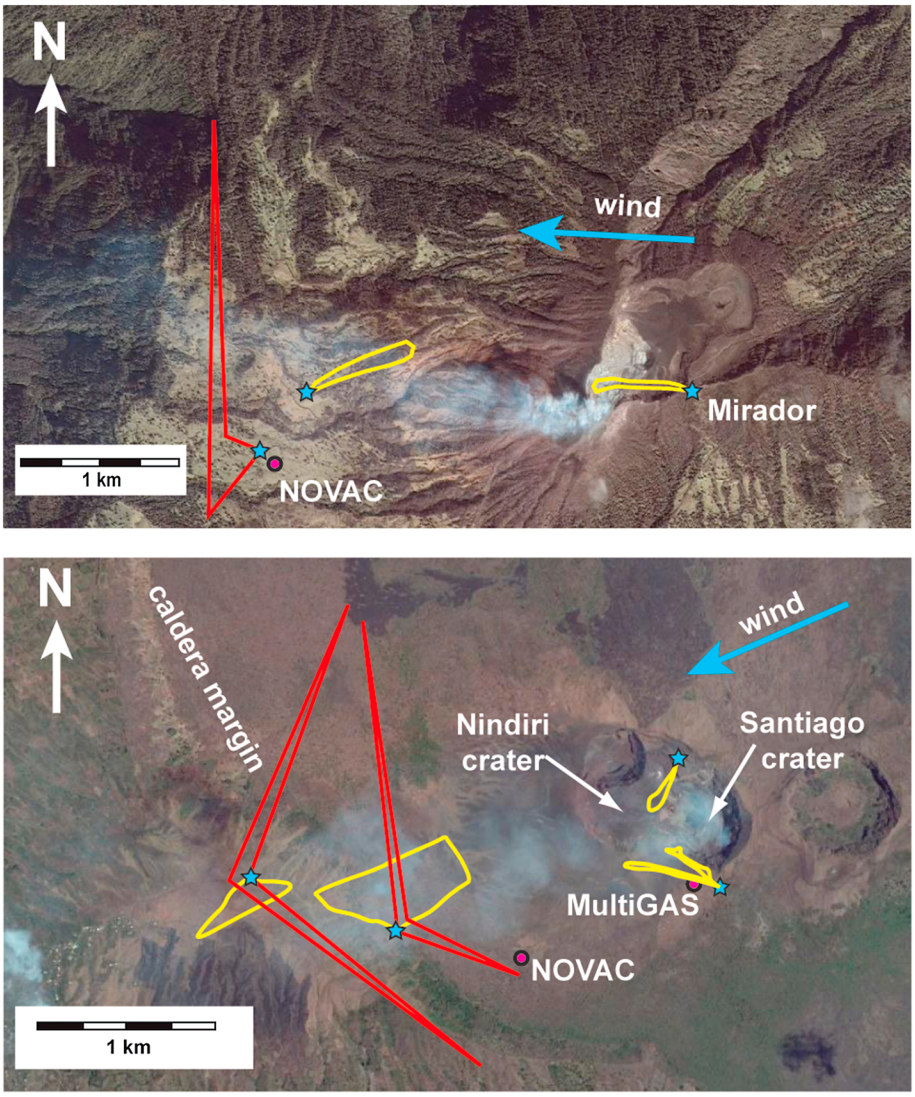

Figure 3. Maps of Turrialba (top) and Masaya (bottom) showing selected flight paths for the drones in 2017. Red paths show programmed flights for DROAS traverses, and yellow paths show manual flights for gas ratio measurements using microGAS and miniGAS. Blue stars show takeoff/landing sites, red dots are gas monitoring stations (either NOVAC or MultiGAS), and blue arrows show wind directions.

acquired only for intergas ratio comparison, rather than retrieval of gas mixing ratios in air. These ground-based samples were analyzed at INGV-Palermo. After sample treatment involving neutralization and oxidation of the sulfur species to sulfate, all samples were analyzed by ion chromatography (IC). Halogen to sulfur ratios were derived by linear regression on a scatter plot of molar concentrations of the respective halogen versus sulfate. In order to estimate halogen fluxes, the halogen to sulfur ratios were multiplied by the SO_2 flux measured by DROAS traverses.

3. Field Methods and Practicalities

We designed our experiment at two volcanoes, Masaya and Turrialba, which in recent years have been the principal contributors to the elevated gas fluxes measured on the Nicaragua-Costa Rica segment of the Central American volcanic arc (de Moor et al., 2017). Both volcanoes are currently in elevated states of activity, with an actively convecting lava lake at Masaya and frequent ash emissions at Turrialba (Global Volcanism Program, 2017a, 2017b). High gas fluxes at these volcanoes provide an ideal testing ground for measurements with drones.

21699356, 2018, 8, Downloaded from https://agupubs.onlinelibrary.wiley.com/doi/10.1029/2018JB015655 by Cochrane Costa Rica, Wiley Online Library on [14/11/2025]. See the Terms and Conditions (https://onlinelibrary.wiley.com/terms-and-conditions) on Wiley Online Library for rules of use; OA articles are governed by the applicable Creative Commons License

Figure 4. Photo showing the DROAS instrument mounted upon the S1000 octocopter. Note that the telescope of the DROAS is angled ~15° from vertical, in order to compensate for the position of the drone when flying, which is tilted slightly forward relative to horizontal.

Masaya is well studied in terms of SO_2 fluxes (Nadeau & Williams-Jones, 2009; Rymer et al., 1998; Stoiber & Williams, 1986) due to easy access conditions allowing DOAS driving traverses at locations 5–10 km from the active crater. However, proximal DOAS transect measurements less than 5 km from the crater are difficult due to lack of roads. Hence, we chose locations between 0 and 5 km from the degassing crater in order to experiment with drone DOAS in these proximal areas (Figure 3). Some of our Masaya data were collected close to the permanent scanning DOAS NOVAC station, in order to directly compare and assess the quality of SO_2 flux data collected by this station with the drone-based data.

Turrialba is less accessible and has higher elevation than Masaya, providing more challenging conditions. Recent degradation of the already rough roads due to devegetation from acid rain, ash, increased runoff, and erosion has made driving DOAS traverses at Turrialba impossible. Hence, drones are a particularly attractive option for continuing traverse DOAS gas flux monitoring at Turrialba for two reasons. First, DROAS traverses along the same trajectory as the preexisting driving traverse database (de Moor et al., 2017) provide consistency and allow for direct comparison with previous measurements (Figure 3). Second, drone measurements are valuable to compare with scanning NOVAC station measurements (Conde et al., 2014; de Moor, Aiuppa, Avard, et al., 2016; de Moor et al., 2017). In particular, drone measurements could help determine plume height (vertical profiles with gas sensors), a parameter which is vital for achieving accurate scanning DOAS measurements (calculated by triangulation between two stations) but usually difficult to quantitatively validate.

Because we were flying our drones on two active volcanoes, both the instruments and the drones were sometimes subjected to difficult field conditions. We developed a fly/no fly checklist which helped us decide if conditions were suitable for flying (Table 2). At Turrialba, SO_2 concentrations sometimes exceeded 100 ppm in the proximal plume, while SO_2 concentrations of 20–30 ppm were commonly encountered at Masaya. Despite these elevated values, the drones and instruments did not suffer noticeable corrosion, probably because flight times were short (typically 10–15 min) and the time spent in the volcanic plume even shorter. In sampling plumes with our MultiGAS instruments, we learned to avoid highly convective and opaque plumes, because such conditions, first, could create strong turbulence for the drone or, second, cause us to lose sight of the drone. Instead, we would pilot the drone carefully toward the margins of the plume, testing and watching its response, and then proceed further into the plume if the drone appeared to be flying stably and the plume was reasonably transparent.

One potential issue is that some drones produce significant electromagnetic interference. In our case, the S1000 drone did produce such interference while the RAVEN did not. The interference was manifested mainly by the infrared analyzers, which produced noisy signals for CO_2 and H_2O, while the electrochemical sensors for SO_2 and H_2S were generally unaffected. We solved this interference problem by encasing the instrumentation in aluminum foil which served as a shield against the interference.

The policies on using drones were different in Costa Rica and Nicaragua. In Costa Rica, we did not experience any regulatory issues since we were flying in an area on and around Turrialba that was closed to public access because of the high activity of the volcano. By contrast, in Nicaragua we were subject to strict regulations imposed by the Instituto Nicaragüense de Aeronáutica Civil (INAC); during the day, INAC personnel accompanied us when we flew, and INAC kept the drones at night for security reasons.

4. Results

4.1. SO_2 Fluxes and Wind Speeds

DROAS traverses were successfully conducted at Turrialba and Masaya volcanoes, and results are reported in Table 3 and Figure 7. Wind speed is a crucial parameter in calculating SO_2 flux from DOAS measurements. In

21699356, 2018, 8, Downloaded from https://agupubs.onlinelibrary.wiley.com/doi/10.1029/2018JB015655 by Cochrane Costa Rica, Wiley Online Library on [14/11/2025]. See the Terms and Conditions (https://onlinelibrary.wiley.com/terms-and-conditions) on Wiley Online Library for rules of use; OA articles are governed by the applicable Creative Commons License

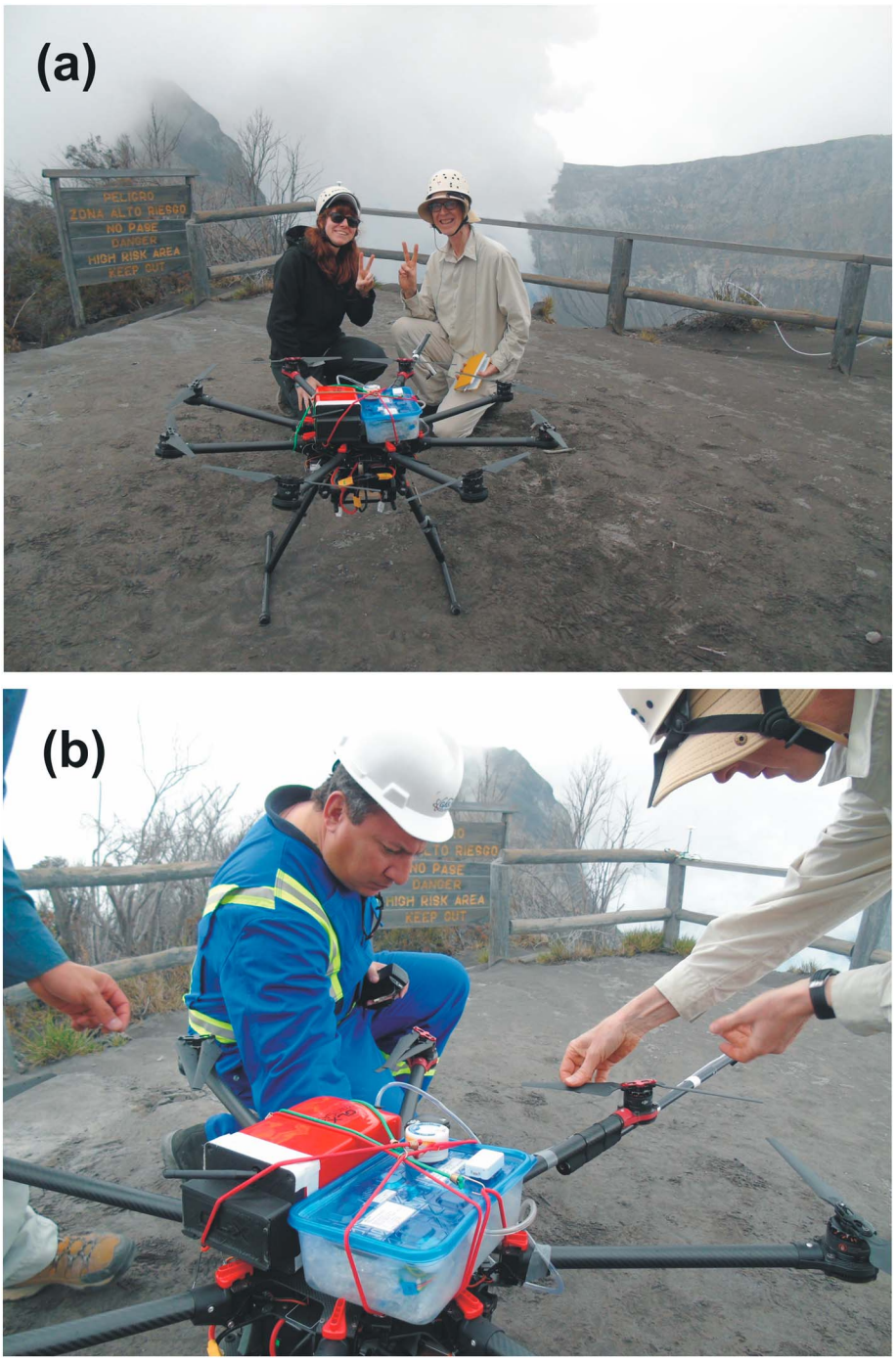

Figure 5. Photos of multiGAS instruments mounted on the S1000 at the summit mirador of Turrialba on 26 April 2017. The miniGAS (red) is mounted on the left, and the microGAS (blue) is mounted on the right. The total payload is ~2 kg.

this study we used a combination of three methods to estimate wind speed, including two vertically positioned DOAS instruments on the ground (Williams-Jones et al., 2006), a Global Forecast System (GFS) at 1° resolution from the NOAA National Center for Environmental Predictions (NCEP; e.g., Conde et al., 2014; de Moor et al., 2017; Hilton et al., 2007), and drone drift measurements. The drone drift measurements consisted of allowing the drone to drift with the wind at plume elevation and recording its change in position with time. Figure 8 shows an example of the drone drift measurement conducted at

21699356, 2018, 8, Downloaded from https://agupubs.onlinelibrary.wiley.com/doi/10.1029/2018JB015655 by Cochrane Costa Rica, Wiley Online Library on [14/11/2025]. See the Terms and Conditions (https://onlinelibrary.wiley.com/terms-and-conditions) on Wiley Online Library for rules of use; OA articles are governed by the applicable Creative Commons License

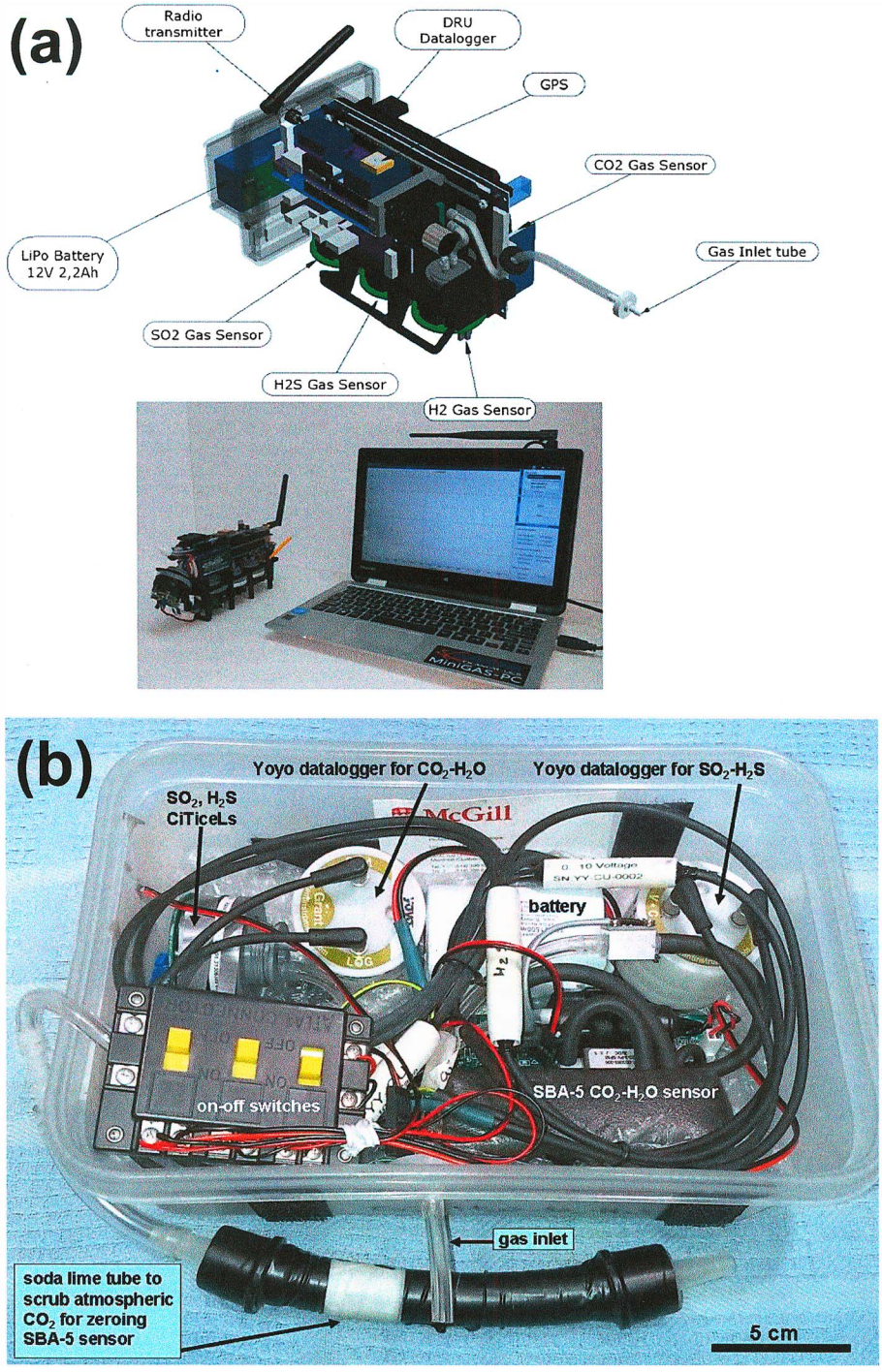

Figure 6. Details of the interior of the (a) miniGAS and (b) microGAS instruments.

Masaya volcano where a wind speed of 7.9 m/s was measured at an altitude of 1,096 m (400 m above ground level). SO_2 concentrations of 1.8 ppm were concurrently measured with miniGAS, indicating that wind speed was determined at true plume level.

Drift speed results are compared to vertical DOAS plume speed measurements and NOAA wind speed measurements in Table 3. Results were consistent between the UAV drift method and the vertical DOAS measurement, with agreement to within 5%. The NOAA GFS data, as well as ground-based

21699356, 2018, 8, Downloaded from https://agupubs.onlinelibrary.wiley.com/doi/10.1029/2018JB015655 by Cochrane Costa Rica, Wiley Online Library on [14/11/2025]. See the Terms and Conditions (https://onlinelibrary.wiley.com/terms-and-conditions) on Wiley Online Library for rules of use; OA articles are governed by the applicable Creative Commons License

Table 2
FLY/NO FLY Criteria

The following list aims to assess whether or not it is safe to fly a drone. Once the list has been completed, a careful risk assessment should be discussed among the flight team.	
Are the winds strong (i.e., more than moderate) with gusts?	YES/NO
Is there a possibility of unexpected turbulence from unusual weather, steep relief, summit areas, hot convecting volcanic gases, eruption columns, etc.?	YES/NO
Are there any physical obstructions present along or near the flight path, that is, crater rims, etc.?	YES/NO
Are the flying distances potentially too great for battery life?	YES/NO
Are the flying distances potentially too great for proper communication?	YES/NO
Is there a potential of losing sight of the drone during its mission?	YES/NO
Are there potential communication issues, that is, static electricity from volcanic ash or gas, clouds present, etc.?	YES/NO
Is the payload potentially too heavy or unstable or unbalanced with respect to the center of gravity on the drone?	YES/NO

measurements of wind speed from the top of the Masaya cone next to the actively degassing crater, typically returned lower wind speed values compared to the drone drift method or the vertical DOAS results. For calculation of SO_2 flux we prefer the UAV drift method, although the vertical DOAS method is equally valid. The benefit of the UAV drift method is that few sources of error exist if the drift is conducted over a sufficient distance. However, gusty conditions can raise issues on how representative one or two drift measurements are. The benefit of the vertical DOAS method is that plume speed data can be acquired continuously over a significant period of time to characterize plume speed variation.

Table 3
Results of Drone-Mounted DOAS (DROAS) Measurements at Turrialba and Masaya Volcanoes

	Method	T/day SO_2	±	Drone drift plume speed	±	2 Vert DOAS plume speed	±	NOAA wind speed	±
Turrialba									
27/4/2017	DROAS flight	1,358	276	na	na	na	na	3.88	0.79
	DROAS flight	1,255	256	na	na	na	na	3.88	0.79
	DROAS flight	1,469	299	na	na	na	na	3.88	0.79
	DROAS flight	1,419	289	na	na	na	na	3.88	0.79
	Average	1,375	280						
Masaya									
4/5/2017	DROAS flight	1,448	71	7.75	0.35	7.51	0.75	3.45	1.01
	DROAS flight	1,041	53	7.75	0.35	7.51	0.75	3.45	1.01
	DROAS flight	1,842	91	7.75	0.35	7.51	0.75	3.45	1.01
	DROAS flight	2,297	112	7.75	0.35	7.51	0.75	3.45	1.01
	Average	1,657	82						
5/5/2017	DROAS flight	1,664	73	8.95	0.35	9.36	0.94	5.47	1.54
	DROAS flight	2,125	102	8.95	0.35	9.36	0.94	5.47	1.54
	DROAS flight	1,773	99	8.95	0.35	9.36	0.94	5.47	1.54
	DROAS flight	1,635	88	8.95	0.35	9.36	0.94	5.47	1.54
	Average	1,799	91						
							na		
6/5/2017	DROAS flight	2,024	59	7.9	0.13	na	na	7.15	1.67
	DROAS flight	1,360	61	7.9	0.13	na	na	7.15	1.67
	DROAS flight	1,547	43	7.9	0.13	na	na	7.15	1.67
	DROAS flight	774	24	7.9	0.13	na	na	7.15	1.67
	Average	1,426	47						
1/5/2017	Driving Traverse	1,561	281	na	na	na	na	5.96	0.90
	Driving Traverse	1,185	231	na	na	na	na	5.96	0.90
	Average	1,373	256						

21699356, 2018, 8, Downloaded from https://agupubs.onlinelibrary.wiley.com/doi/10.1029/2018JB015655 by Cochrane Costa Rica, Wiley Online Library on [14/11/2025]. See the Terms and Conditions (https://onlinelibrary.wiley.com/terms-and-conditions) on Wiley Online Library for rules of use; OA articles are governed by the applicable Creative Commons License

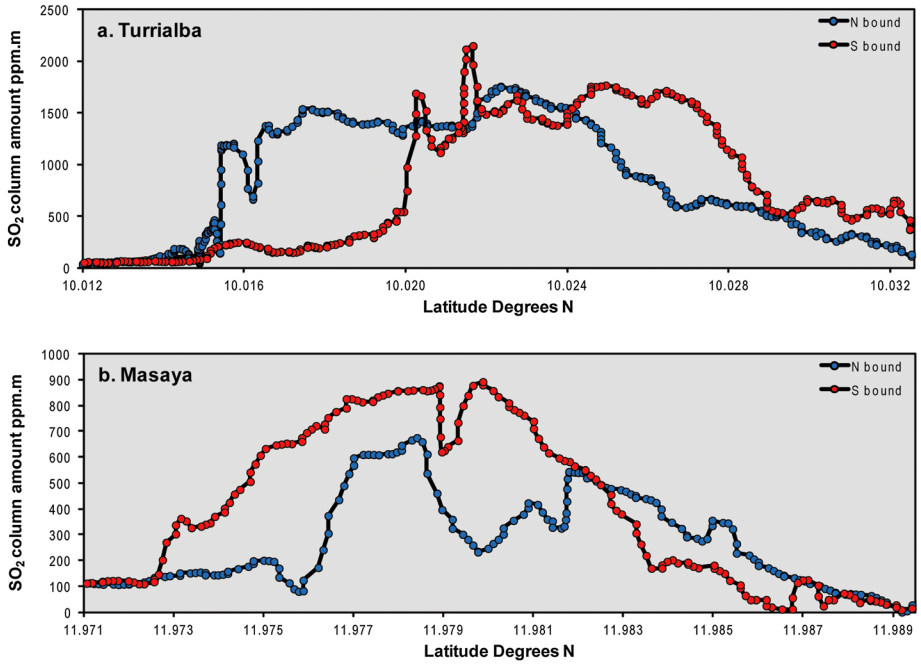

Figure 7. Plot of SO_2 column amounts for DROAS traverses at (a) Turrialba and (b) Masaya in April–May 2017. Each plot shows two traverses, one outbound and the other inbound. Note the excellent temporal resolution of the data and the complexity of the plumes, which changes over short periods of time.

Errors associated with the vertical DOAS method are mostly geometric, relating to (a) positioning of the two vertically pointing instruments relative to the plume travel direction, and (b) precise mounting of the DOAS telescope in a perfectly vertical position. The errors are reduced if the plume is low and the distance between the two DOAS instruments is large. Comparison among UAV drift, two vertical DOAS instruments, and NOAA wind speeds shows that the latter significantly underestimates plume speeds by 40% to 55%.

The SO_2 flux measured at Turrialba on 27 April 2017 was 1,380 ± 280 T/day (Table 3). The average SO_2 flux for Turrialba reported by de Moor et al. (2017) for 2015 and 2016, a period of elevated degassing

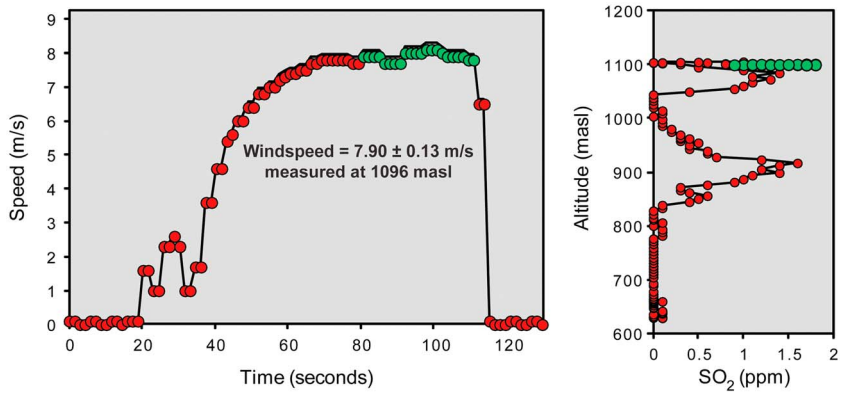

Figure 8. Example of a wind speed calculation using the drift of the drone at Masaya in May 2017 (left) with SO_2 concentration profile showing the main plume at 1,100 m and a secondary peak at 900 m possibly due to plume puffing (right). The drone is flown to the altitude of the gas plume, where it is allowed to drift with the wind. After ~60 s the speed of the drone stabilizes, which we consider to be the true wind speed at plume height. The calculations are done using the Global Positioning System data of the drone and our instruments.

21699356, 2018, 8, Downloaded from https://agupubs.onlinelibrary.wiley.com/doi/10.1029/2018JB015655 by Cochrane Costa Rica, Wiley Online Library on [14/11/2025]. See the Terms and Conditions (https://onlinelibrary.wiley.com/terms-and-conditions) on Wiley Online Library for rules of use; OA articles are governed by the applicable Creative Commons License

Journal of Geophysical Research: Solid Earth

10.1029/2018JB015655

Table 4
Gas Ratios Measured at Turrialba and Masaya by MiniGAS and MicroGAS

Volcano	Date	Local time	Data type	Instrument	Maximum SO_2	CO_2/SO_2	R^2	H_2O/SO_2	R^2	H_2O/CO_2	R^2	Notes
		(hr)			(ppm)							
Turrialba	26 Apr 2017	1159–1204	drone	microGAS	115	6.31	0.94	27.8	0.95			
Turrialba	26 Apr 2017	1159–1204	drone	microGAS + miniGAS	115	6.70	0.91					SO_2 from microGAS, CO_2 from miniGAS
Turrialba	26 Apr 2017	1310–1317	drone	miniGAS	152	6.56	0.93					
Turrialba	28 Apr 2017	0952–0958	drone	microGAS	6.9	7.64	0.91					
Turrialba	28 Apr 2017	1101–1106	ground	microGAS	2.0	7.50	0.90					data collected on ground in valley
Masaya	1 May 2017	1110–1115	ground	microGAS	34	4.11	0.87	55.6	0.95	11.8	0.84	edge of Santiago crater in Nindirí
Masaya	1 May 2017	1237–1240	ground	microGAS	6	4.44	0.89					edge of Santiago crater in Nindirí
Masaya	1 May 2017	1255–1305	ground	microGAS	19	3.98	0.86					edge of Santiago crater in Nindirí
Masaya	1 May 2017	1412–1418	ground	microGAS	15	4.54	0.90					edge of Santiago crater in Nindirí
Masaya	1 May 2017	1118–1120	ground	microGAS	1.2	27.0	0.84					edge of Santiago crater in Nindirí
Masaya	1 May 2017	1207–1209	ground	microGAS	3.3	50.0	0.72					edge of Santiago crater in Nindirí
Masaya	1 May 2017	1500–1502	ground	microGAS	2.0	38.4	0.89					edge of Santiago crater in Nindirí
Masaya	2 May 2017	1017–1033	ground	microGAS	19	3.49	0.78					edge of Santiago crater in Nindirí
Masaya	2 May 2017	1050–1102	ground	microGAS	28	3.42	0.80	63.6	0.77			edge of Santiago crater in Nindirí
Masaya	2 May 2017	1107–1112	ground	microGAS	18	3.54	0.84	52.3	0.94	13.0	0.79	edge of Santiago crater in Nindirí
Masaya	2 May 2017	1135–1148	ground	microGAS	30	3.51	0.76					edge of Santiago crater in Nindirí
Masaya	3 May 2017	1542–1551	drone	miniGAS	23.7	2.06	0.69					
Masaya	4 May 2017	1037–1050	drone	microGAS	31	3.50	0.83	78.7	0.79			
Masaya	4 May 2017	1103–1113	drone	microGAS	34	3.68	0.84	61.5	0.82	13.8	0.80	
Masaya	4 May 2017	1125–1136	drone	miniGAS	14.1	2.92	0.76					
Masaya	5 May 2017	0933–0942	drone	microGAS	15	3.92	0.94					
Masaya	5 May 2017	1019–1028	drone	miniGAS	17	2.00	0.84					
Masaya	5 May 2017	~1203	drone	miniGAS	9.3	1.89	0.84					
Masaya	5 May 2017	1240–1251	drone	microGAS	11	4.34	0.89					
Masaya	5 May 2017	1628–1640	drone	miniGAS	4.1	1.37	0.86					
Masaya	6 May 2017	1118–1130	drone	microGAS	2.5	6.20	0.77					distal flight near caldera margin
Masaya	6 May 2017	1148–1201	drone	miniGAS	1.7	4.10	0.86					distal flight near caldera margin
Masaya	6 May 2017	1305–1315	drone	microGAS	3.4	4.62	0.72					distal flight near caldera margin

Note. For H_2O/SO_2 and H_2O/CO_2 ratios, the blank spaces indicate that the microGAS instrument was unable to measure H_2O. The miniGAS instrument did not have a H_2O sensor.

21699356, 2018, 8, Downloaded from https://agupubs.onlinelibrary.wiley.com/doi/10.1029/2018JB015655 by Cochrane Costa Rica, Wiley Online Library on [14/11/2025]. See the Terms and Conditions (https://onlinelibrary.wiley.com/terms-and-conditions) on Wiley Online Library for rules of use; OA articles are governed by the applicable Creative Commons License

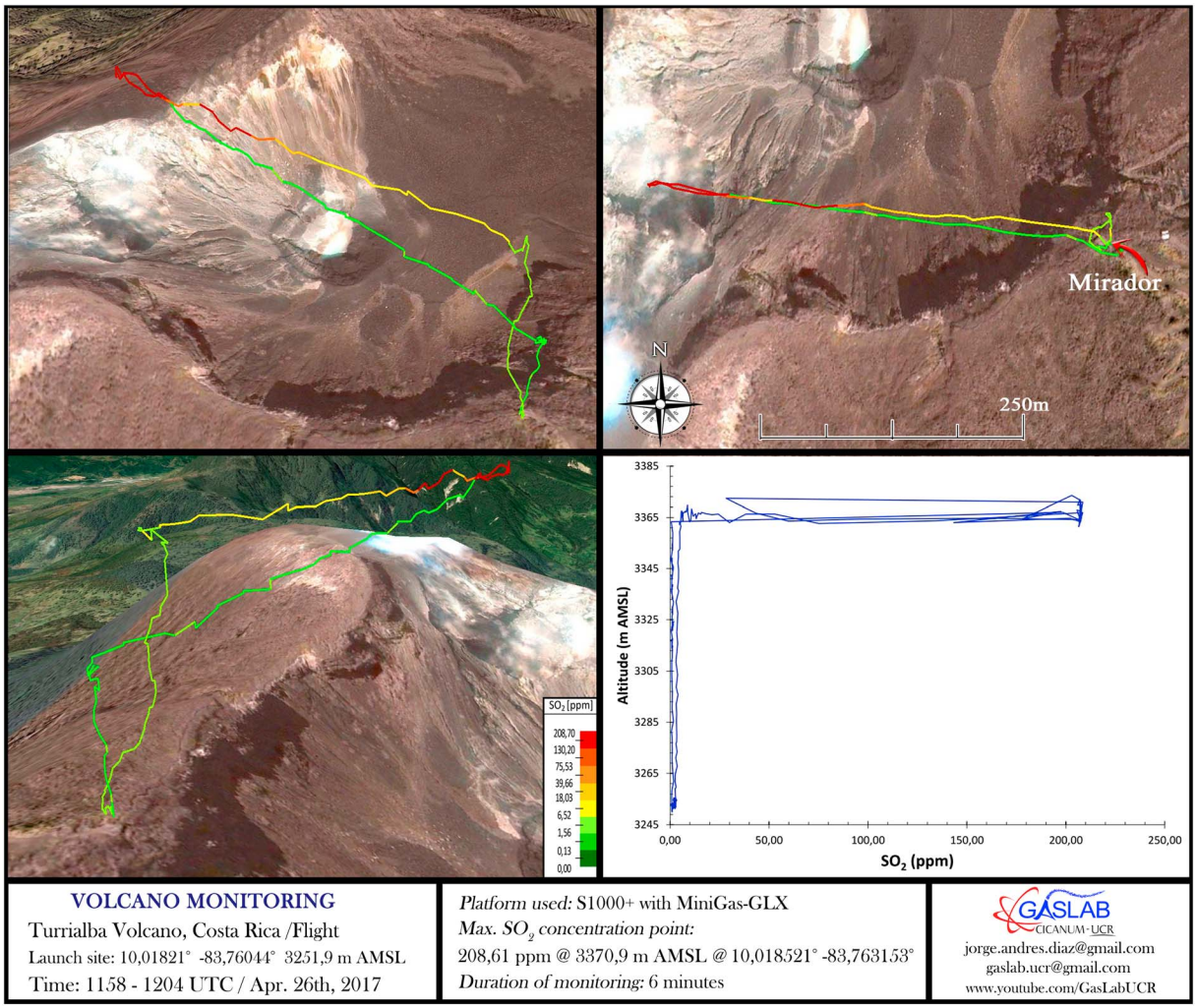

Figure 9. UAV flight from the mirador into the crater of Turrialba on 26 April 2017. The flight is recorded from three perspectives, with SO_2 concentrations shown by the color scheme from lowest (dark green) to highest (red). The lower right panel shows SO_2 concentrations as a function of altitude.

and eruptive activity, was 2,990 ± 980 T.day. Within this context, our DROAS measurement could be interpreted to reflect either decreased sulfur degassing compared to 2015–2016 or a partially constricted conduit prior to the new eruptive period that began at Turrialba on 11 May 2017 and continued through mid-July 2017.

The SO_2 fluxes measured at Masaya by DROAS on 5 May 2017 were between 1,300 and 1,900 T/day and averaged 1,560 ± 120 T/day (Table 3), in agreement with driving DOAS traverses conducted in the traditional manner (1,370 ± 260 T/day on 1 May 2017). The average SO_2 flux reported at Masaya for 2015–2016 by de Moor et al. (2017) was 1880 ± 510 T/day. Our DROAS measurements at Masaya are thus consistent with a relatively steady state volatile flux from Masaya.

4.2. SO_2, CO_2, and H_2O Concentrations, Ratios, and Derived Fluxes

Gas ratios were successfully measured at both volcanoes, and results are shown in Table 4. On 26 April 2017 at Turrialba, we flew our drones from the Mirador at ~3,250 m directly into the degassing crater which was several hundred meters distant (Figure 9). Maximum measured gas concentrations were 152 ppm SO_2, 1,712 ppm CO_2, and 21,270 ppm H_2O (the water background varied from ~16,250 to ~17,000 ppm). Using two independent arrays of gas sensors (miniGAS and microGAS), we consistently measured CO_2/SO_2 ratios of 6.3–6.7 in the plume gas of the crater (Table 4 and Figure 10). We also measured a

21699356, 2018, 8, Downloaded from https://agupubs.onlinelibrary.wiley.com/doi/10.1029/2018JB015655 by Cochrane Costa Rica, Wiley Online Library on [14/11/2025]. See the Terms and Conditions (https://onlinelibrary.wiley.com/terms-and-conditions) on Wiley Online Library for rules of use; OA articles are governed by the applicable Creative Commons License

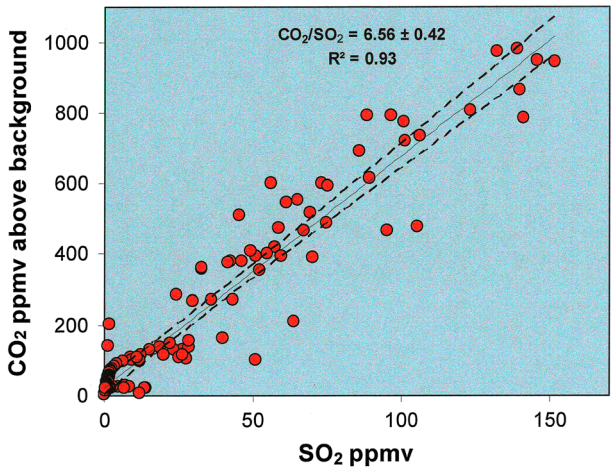

Figure 10. Plot of SO_2 versus CO_2 for miniGAS data from a drone flight at Turrialba on 26 April 2017. Note the elevated CO_2/SO_2 ratio and the excellent R^2 value.

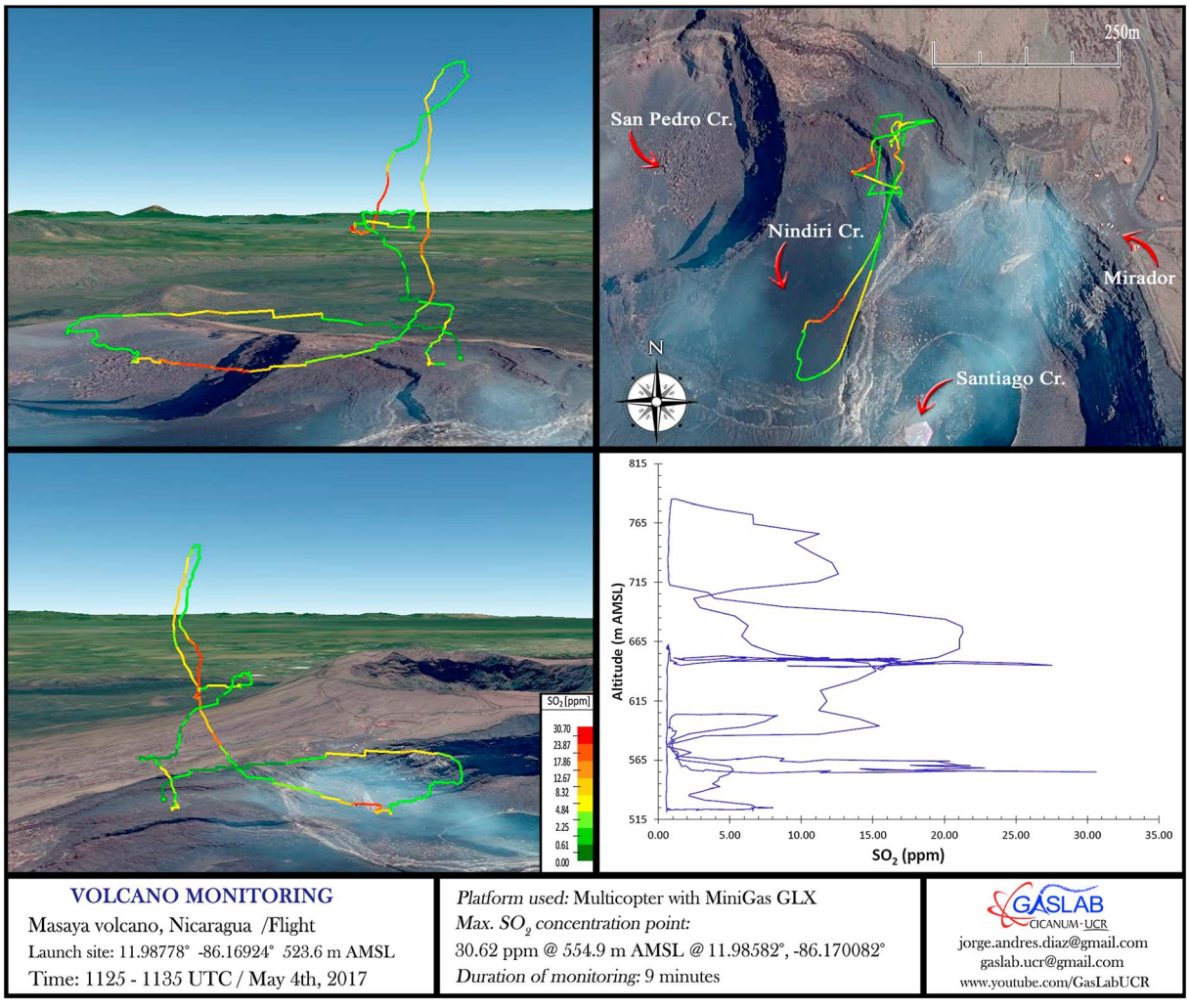

Figure 11. UAV flight at Masaya on 4 May 2017. The flight is recorded from three perspectives, with SO_2 concentrations shown by the color scheme from lowest (dark green) to highest (red). The lower right panel shows SO_2 concentrations as a function of altitude.

21699356, 2018, 8, Downloaded from https://agupubs.onlinelibrary.wiley.com/doi/10.1029/2018JB015655 by Cochrane Costa Rica, Wiley Online Library on [14/11/2025]. See the Terms and Conditions (https://onlinelibrary.wiley.com/terms-and-conditions) on Wiley Online Library for rules of use; OA articles are governed by the applicable Creative Commons License

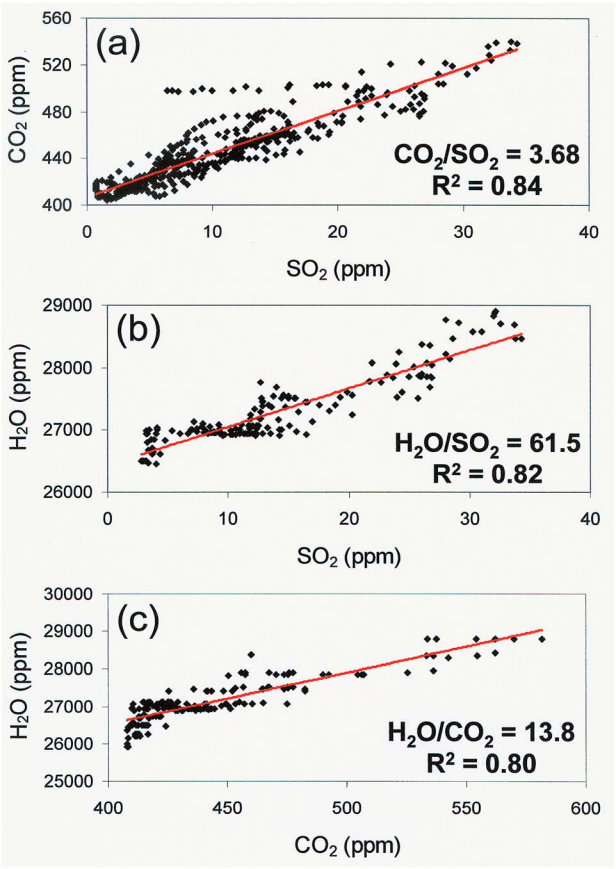

Figure 12. Plot of microGAS data from a drone flight at Masaya on 4 May 2017. (a) SO_2 versus CO_2; (b) H_2O versus SO_2; (c) H_2O versus CO_2. A high degree of correlation can be seen for all plots, attesting to the elevated gas concentrations in the plume and the excellent sensitivity of the instruments.

single H_2O/SO_2 ratio of 27.8, with an R^2 value of 0.95. On 28 April we made one flight 1–2 km west of the crater and measured maximum SO_2 of 6.9 ppm, maximum CO_2 of 460 ppm, and CO_2/SO_2 of 7.6, while a ground measurement an hour later yielded maximum SO_2 of 2.0 ppm, maximum CO_2 of 429 ppm, and CO_2/SO_2 of 7.5. These ratios are slightly higher than those on 26 April. No water measurements were possible for 28 April. H_2S was below detection limit of the method at Turrialba, consistent with the disappearance of this gas in 2015 with the transition from phreatic to magmatic conditions (de Moor, Aiuppa, Avard, et al., 2016).

At Masaya, measurements were made on 1–6 May. On 1–2 May we made stationary measurements at the edge of Santiago crater, while on 3–6 May we made drone measurements at various distances from the crater (Figures 3 and 11). The two CO_2-SO_2 sensor arrays showed slightly different results. The first array (miniGAS) returned CO_2/SO_2 ratios of 1.4–4.1, while the second array (microGAS) returned CO_2/SO_2 of 3.4–6.2 (Table 4 and Figure 12a). For days with simultaneous measurements, the two arrays respectively measured CO_2/SO_2 of 2.9 and 3.5–3.7 (4 May), 1.4–2.0 and 3.9–4.3 (5 May), and 4.1 and 4.6–6.2 (6 May). The 6 May measurements were comparatively distal, located on the edge of the caldera ~3 km west and downwind from the degassing crater. At this location SO_2 concentrations typically were 2–3 ppm compared to measurements closer to the crater where SO_2 concentrations reached 34 ppm. No H_2S was detected at Masaya, which is consistent with previous MultiGAS studies (Aiuppa et al., 2018; de Moor et al., 2017) and the absence of hydrothermal processes.

At Masaya, it is possible to make a comparison of the ground-based and drone data. On 1–2 May, stationary ground-based measurements were made at the edge of Santiago crater (Figure 3). Maximum SO_2 concentrations were mostly 15–34 ppm, with several lower values. These comparatively high concentrations resulted in very good correlations between SO_2 and CO_2, with nearly all R^2 values >0.8 (Table 4). Drone flights on 4–6 May were at different distances from the crater. On 4–5 May, the drones were flown over Nindirí crater close to Santiago, while the 6 May flights were made from the edge of the caldera ~3-km distant from Santiago (Figure 3). Maximum SO_2 concentrations on 4 May were 14–34 ppm, similar to 1–2 May, and R^2 values for CO_2/SO_2 ratios were 0.76–0.84 (Figure 12a). On 5 May maximum SO_2 was lower (4.1–17 ppm), but R^2 values all exceeded 0.8. Most importantly, CO_2/SO_2 ratios for these dates were very similar (1–2 May 3.4–4.5, 4 May 3.5–3.7, 5 May 3.9–4.3, all data from microGAS; Table 4). On 6 May, maximum SO_2 was low (1.7–3.4 ppm) because of plume dilution, yet R^2 values were only slightly degraded (0.72–0.86). We conclude that both the ground-based and drone measurements produce high-quality data, with the drone measurements comparable to the ground measurements. Furthermore, data quality by drone is maintained at low SO_2 concentrations (<5 ppm). One reason for this is that the drone measurements produced a simple peak or series of peaks for SO_2 and CO_2 concentrations. The backgrounds also were generally very stable, with SO_2 essentially at zero and CO_2 at 400–410 ppm. These conditions allowed robust comparisons and correlations between CO_2 and SO_2.

Several ground-based Masaya data sets from 1 May taken at the edge of Santiago crater show anomalously high CO_2/SO_2 ratios of 27–50, which were observed at low SO_2 contents of 1–3 ppm (Table 4). The correlations between the two gases are generally very good, with R^2 values of 0.72–0.89. No such high values were measured by drone. The elevated ratios are likely the result of contamination of the plume by diffuse degassing along the edge of Santiago crater. The diffuse degassing releases CO_2 but no SO_2. Hence, a clear advantage of drone-based measurements over those made on the ground is the ability to sample a gas plume without contamination from diffusely degassing sources.

21699356, 2018, 8, Downloaded from https://agupubs.onlinelibrary.wiley.com/doi/10.1029/2018JB015655 by Cochrane Costa Rica, Wiley Online Library on [14/11/2025]. See the Terms and Conditions (https://onlinelibrary.wiley.com/terms-and-conditions) on Wiley Online Library for rules of use; OA articles are governed by the applicable Creative Commons License

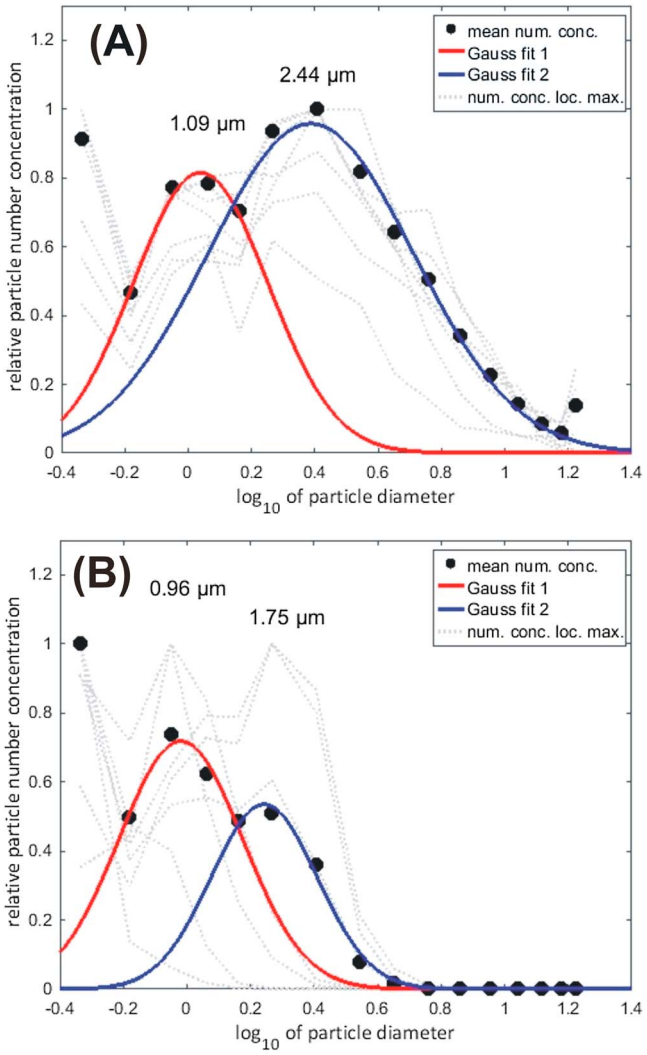

Figure 13. Particle size distribution observed at proximal and distal locations at Masaya in May 2017. (a) Size distribution in the plume at the rim of Santiago crater on 2 May 2017 (ground-based data). (b) Size distribution in the plume above the western caldera wall ~3 km distant from Santiago crater on 6 May 2017 (drone data). Both data sets show two particle modes. The proximal data from the crater show the two identified particle modes with larger mean diameter and the larger particle mode with a relative higher concentrations compared to the distal caldera edge data.

At Masaya we were also able to precisely measure H_2O/SO_2 and H_2O/CO_2 ratios (Table 4 and Figures 12b and 12c). For H_2O/SO_2, on 1 May we obtained a single value of 55.6 (R^2 0.95), and on 2 May two values of 63.6 and 52.3 (R^2 0.77, 0.94). These were proximal ground-based measurements at the edge of Santiago crater (Figures 3 and 11). On 4 May we measured two values of 78.7 and 61.5 (R^2 0.79, 0.82) by drone above Nindirí (Figures 3 and 12b). Hence, the range was 52.3–78.7, and the average H_2O/SO_2 was 62.3.

For H_2O/CO_2, our ground measurements on 1–2 May gave values of 11.8 and 13.0 (R^2 0.84, 0.79) at the crater edge, while a drone-based measurement on 4 May gave a value of 13.8 (R^2 0.80; Table 4 and Figure 12c). Hence, the ground-based and drone-based measurements were highly consistent. Typical water backgrounds were 26,000–27,000 ppm, with water peaks ~1,700–1,900 ppm higher than the background.

At Turrialba, using a CO_2/SO_2 ratio of 6.5 and a H_2O/SO_2 ratio of 27.8 obtained on 26 April and the SO_2 flux of 1,380 T/day obtained on 27 April, we calculate a CO_2 flux of 6,170 T/day and a H_2O flux of 10,790 T/day. For Masaya, we used an average SO_2 flux of 1,560 T/day, an average CO_2/SO_2 of 3.9, and an average H_2O/SO_2 of 62.3 to calculate average CO_2 and H_2O fluxes of 4,150 T/day and 27,330 T/day, respectively. We also used our minimum and maximum ratios and fluxes at Masaya to calculate the possible ranges of CO_2 and H_2O fluxes, which were 3,140–5,570 T/day and 19,120–42,060 T/day, respectively.

4.3. Aerosols

Particle data were collected in proximal environments on two days. At Turrialba on 26 April we measured particle concentrations of the gas plume in the crater with a drone, while at Masaya on 2 May we made stationary measurements on the edge of Santiago crater. Evaluation of the particle size distribution for the stationary measurement at Masaya showed two modes, one at 1.09 μm and the second at 2.44 μm, which is the more prominent mode at this location (Figure 13a). The sized distribution also indicates that other modes outside the measurement range of the optical particle counter may have been present. An increase in the particle numbers toward the edges of the distribution was observed. For these dates, particle concentrations were generally very high, with PM1, PM2.5, and PM10 values reaching 8.7×10^2, 5.4×10^3, and 4.3×10^4 μg m^{-3}, respectively. As a result, PM10/PM2.5, PM10/PM1, and PM2.5/PM1 ratios were 4, 43, and 11 at Turrialba and 24, 103, and 4.5 at Masaya.

At Masaya we also collected particle data at more distant locations from the crater. On 4–5 May measurements were made by drone through the plume at a distance of 200–300 m from the degassing crater. These results showed substantially lower PM10 values which did not exceed 1.5×10^3 μg m^{-3}. Hence, PM10/PM2.5, PM10/PM1, and PM2.5/PM1 ratios were 1.0–1.1, 1.3–1.5, and 1.2–1.4. On May 6 we made distal measurements ~3 km downwind from the crater. During two flights the plume was intersected 3 times, as indicated by elevated particle counts. The particle size distribution for the drone-based measurements showed that again two modes were observable (Figure 13b). The mean diameters of these modes were 0.96 μm and 1.75 μm. In contrast to the measurements at the crater rim, the normalized number concentration (dN/dlogDp) of the smaller mode was determined to be higher than that of the larger particles (Figure 13). Relative to 4–5 May, PM10 concentrations showed an increase to a maximum of 3.7×10^3 μg/m^3, which corresponds to slightly higher PM10/PM2.5, PM10/PM1, and PM2.5/PM1 ratios of 1.0–1.5, 1.7, and 1.6–1.7, respectively.

21699356, 2018, 8, Downloaded from https://agupubs.onlinelibrary.wiley.com/doi/10.1029/2018JB015655 by Cochrane Costa Rica, Wiley Online Library on [14/11/2025]. See the Terms and Conditions (https://onlinelibrary.wiley.com/terms-and-conditions) on Wiley Online Library for rules of use; OA articles are governed by the applicable Creative Commons License

21699356, 2018, 8, Downloaded from https://agupubs.onlinelibrary.wiley.com/doi/10.1029/2018JB015655 by Cochrane Costa Rica, Wiley Online Library on [14/11/2025]. See the Terms and Conditions (https://onlinelibrary.wiley.com/terms-and-conditions) on Wiley Online Library for rules of use; OA articles are governed by the applicable Creative Commons License

4.4. Halogen Concentrations and Fluxes

At Masaya four alkaline trap samples were obtained between 1 and 4 May 2017 at the rim of Santiago crater. On 1 May a Raschig tube sample was taken, while on the following days only Drechsel bottles were used. All samples were analyzed by ion chromatography, and a molar HCl/SO_2 ratio of 0.59 (R^2 = 0.985, n = 4) was derived. From that an average HCl flux of 519 ± 62 T/day was calculated using the average SO_2 flux from Masaya volcano during the field campaign.

5. Discussion

Drone-based DOAS traverses provide a highly flexible and robust method for accurately measuring SO_2 fluxes. First, flights are quick, allowing rapid transects below dynamic plumes. Driving or walking DOAS traverses can take a long time, during which plumes can change direction or intensity. Furthermore, drones are not restricted by road access, allowing traverse measurements to be conducted under virtually any wind direction and intensity (except very high wind conditions with winds >15 m/s). Geometric errors are also reduced by linear flight paths (Figures 3 and 7). DROAS measurements record full spectral information, allowing detailed post-processing of the data to assess, for example, SO_2 column amount retrievals as a function of fit window (Kern et al., 2009). Since data processing of DROAS traverses is rapid, SO_2 flux estimates can be quickly extracted shortly after data acquisition, which is important for hazard assessment during volcanic crises. Wind speed, a crucial parameter and the largest source of error in SO_2 flux estimation, can also be directly measured at plume height by drone. One potential issue with DROAS traverses is that the drone needs to fly as low as possible in order to capture the whole plume above it. This was not an issue during our DROAS measurements, as a negligible amount of SO_2 was detected close to the ground using multiGAS. However, this need to fly low may be an issue with ground-hugging plumes or with certain topographic and atmospheric conditions.

Our work at Masaya demonstrates that drone-based measurements of gas concentrations and ratios produce results which are comparable to ground-based measurements in terms of accuracy and precision. The data quality remains excellent from high gas concentrations (e.g., 30 ppm SO_2) to low gas concentrations (< 5 ppm). Other workers have shown that drone-based instrumentation can measure subpart per million concentrations in some cases (Mori et al., 2016). The ability of a drone to sample discrete regions of a volcanic plume produces a wide range of gas concentrations, which are well correlated. So long as electromagnetic interference produced by the drone can be minimized or eliminated, the drone data are high quality and reliable.

5.1. SO_2 Fluxes From Turrialba and Masaya

Masaya is the largest long-term time-integrated gas emitter in Central America (Andres & Kasgnoc, 1998; Mather et al., 2006). Turrialba volcano reactivated in the mid 2000s and now rivals Masaya as the largest emitter of SO_2 in Central America (de Moor et al., 2017). Our SO_2 flux data, the first published for these volcanoes for 2017, show that gas fluxes remain high at both and are of similar magnitude (Table 3). De Moor et al. (2017) showed that Masaya and Turrialba together account for ~78% of the SO_2 flux from volcanic degassing in Costa Rica and Nicaragua. Our data show that the combined SO_2 flux from Masaya and Turrialba was 2,940 ± 460 T/day in April–May 2017, which is somewhat lower than the 2015–2016 fluxes at these volcanoes (4,870 ± 1,490 T/day) (de Moor et al., 2017). This is mainly due to lower flux measured at Turrialba in the present study. Our data highlight the variability of gas emission rates at dynamic volcanoes. Our average SO_2 flux of 1,560 ± 120 T/day from Masaya is significantly higher than the SO_2 fluxes derived from NOVAC scanning DOAS instruments reported in Aiuppa et al. (2018), where an average SO_2 flux of 690 ± 260 T/day was reported during lava lake activity from NOVAC measurements. This demonstrates that careful evaluation is essential for scanning DOAS measurements, which are subject to more errors than traverse measurements and most likely underestimate SO_2 fluxes (de Moor et al., 2017).

5.2. Gas Compositions and Outputs From Turrialba and Masaya

The gases currently emanating from Turrialba appear to be unusual in three ways: (1) no H_2S is present, (2) the CO_2/SO_2 ratios that we measured are comparatively elevated, and (3) our measured H_2O/SO_2 ratio is the highest recorded in the past several years (de Moor et al., 2017). These observations suggest that the

21699356, 2018, 8, Downloaded from https://agupubs.onlinelibrary.wiley.com/doi/10.1029/2018JB015655 by Cochrane Costa Rica, Wiley Online Library on [14/11/2025]. See the Terms and Conditions (https://onlinelibrary.wiley.com/terms-and-conditions) on Wiley Online Library for rules of use; OA articles are governed by the applicable Creative Commons License

magmas and gases now feeding Turrialba are magmatic in nature and rich in both water and carbon as well as sulfur. Such conditions suggest that the current unrest at Turrialba will continue in the foreseeable future and could escalate. The relatively low SO_2 fluxes that we measured could be indicative of a conduit that is partially blocked. Shortly after our measurements, Turrialba entered an ash emission episode, which lasted from 9 May to 10 July 2017. This change may indicate a change from partially blocked to more open conditions within the conduit system.

At Masaya, our results can be compared with long-term monitoring by a ground-based MultiGAS network. The recent work of Aiuppa et al. (2018) reveals that CO_2/SO_2 and H_2O/CO_2 at Masaya underwent significant changes associated with the development of the lava lake in Santiago crater in December 2015. CO_2/SO_2 demonstrated a clear increase from mean values around 5 to >12 about 2 to 3 weeks before the lava lake was first observed, then dropped to values of ~5.5 when the lava lake was established. H_2O/CO_2 showed a substantial decrease prior to and during lava lake emergence, from mean values around 17 beforehand to values <5 during lake formation. By the second half of 2016 and the first quarter of 2017, H_2O/CO_2 had increased appreciably to a mean value of ~13. De Moor et al. (2017) showed that during the second half of 2016, mean CO_2/SO_2 was 4.0 with a range of 3.1–4.8, while mean H_2O/SO_2 was 65 with a range of 47–98. Our CO_2/SO_2, H_2O/SO_2, and H_2O/CO_2 data, measured both by drone and on the ground, are fully consistent with these independent observations.

Turrialba and Masaya are the major sources of gas output in the southern Central American Volcanic Arc. Despite the somewhat lower SO_2 fluxes relative to previous measurements in the past several years (de Moor et al., 2017), the combined fluxes that we measured from these volcanoes are nearly 3,000 T/day SO_2, ~10,000 T/day CO_2, and ~38,000 T/day H_2O. The elevated SO_2, CO_2, and water fluxes reflect both the high level of unrest at both systems (continued ash emission at Turrialba and an actively convecting lava lake at Masaya) and the underlying magmas which are themselves rich in sulfur, carbon, and water.

5.3. Aerosols at Turrialba and Masaya

A comparison of particle size distributions at Masaya obtained during the crater rim measurements and the distal flights shows a loss of larger particles, which becomes apparent by the shift in the size distribution toward smaller particles, the decrease of the larger particle mode and omission of the particle fraction in the 16.75 μm fraction (Figure 13). This is probably due to the deposition of the larger fraction of particles in the coarse mode, which are typically associated with a primary origin. At the crater rim larger particles may be produced by a gas bubble-bursting mechanism and then deposited downwind. The proximal particle measurements made on 26 April at Turrialba and on 2 May at Masaya reveal elevated PM10 concentrations, commonly exceeding 10^4 μg/m^3 and significantly higher than PM1 and PM2.5 concentrations. These very high values likely reflect the high levels of activity at both volcanoes when the measurements were made. At Turrialba, ash emissions were occurring on a regular basis in April 2017, and we observed these emissions on 26 April. Hence, the elevated PM10 values at Turrialba probably include a portion of fine ash. At Masaya, the lava lake was strongly convecting at the time of our measurements, with intense degassing including frequent bubble bursts. Such activity is likely to produce comparatively large, glassy, silicate microspheres, which have been previously noted at Masaya (Martin et al., 2012; Moune et al., 2010) and elsewhere (e.g., Erta Ale, Zelenski et al., 2013). The significant decrease in PM10 concentrations outside the crater areas of both volcanoes are the result of sedimentation of the large particles in comparatively proximal environments.

6. Concluding Remarks

The main conclusions of this study are the following:

1. Miniaturized (~1 kg) gas instrumentation mounted on low-cost drones has enormous potential for safely, rapidly, accurately, and precisely characterizing the gas output of a volcano at all stages of activity. If done carefully, such measurements can be made even when the volcano is erupting. Such an approach allows an excellent snapshot of the current degassing state of an active volcano.
2. Gas ratios and SO_2 fluxes can be measured by drone with data quality comparable to other methods. The rapid introduction of a drone into high-concentration gas for several minutes generates highly linear and correlated gas concentrations to calculate ratios of high accuracy and precision. Drone flights beneath a plume allow controlled DROAS traverses perpendicular to the plume, with a high level of detail in terms of

the SO_2 concentration profile, as well as accurate wind speed measurements when the drone is allowed to drift parallel to the plume at the same altitude. Drones also can efficiently acquire particle and aerosol size distribution data which can be directly compared to the gas data.

3. Our results demonstrate that at the time of our measurements Turrialba was releasing magmatic gases that were comparatively rich in H_2O and CO_2. The CO_2/SO_2 ratios that we measured are comparatively elevated, while our measured H_2O/SO_2 ratio is the highest yet observed in the past several years. These indicators show that the volcano is being fed by magma enriched in water and carbon. The somewhat low SO_2 fluxes that we observed may be of concern if they are indicating a partially blocked conduit system. This potential blocking, together with the gas compositions we observed, suggests a system which is active and potent. Shortly after our measurements in 2017, Turrialba entered an eruptive phase that lasted several months.
4. The Masaya data reveal that the development of the lava lake in Santiago crater since late 2015 is now associated with stable CO_2/SO_2 and H_2O/SO_2 ratios, with CO_2/SO_2 currently at relatively low levels and H_2O/SO_2 at comparatively high levels.

Our work demonstrates the importance of continued and continual gas measurements at these highly active systems. The near-term future evolution of Turrialba is a crucial yet unanswered question in terms of hazards specific to this volcano, and more generally as well for other volcanoes with long periods of unrest (i.e., several decades). At Masaya, understanding future magma movements and associated gas release is directly relevant to hazards, public health, and scientific understanding of highly convective magmatic systems.

Acknowledgments

We thank Ryunosuke Kazahaya and one anonymous reviewer for careful and detailed comments and suggestions, which allowed us to make significant and substantive improvements to this paper. We also thank Sandro Aiuppa for helpful discussions on gas emissions at Masaya. J. S. and F. D. have been supported by Discovery, Accelerator, and CREATE grants from the Natural Sciences and Engineering Research Council of Canada. J. M. d M. acknowledges support from the Deep Carbon Observatory, including from the Biology Meets Subduction project, and funding from the Ley Transitorio 8933. J. R. acknowledges support by the German Academic Exchange Service (DAAD). The GasLab team would like to acknowledge the support of the Dean of Research office (Vicerrectoria de Investigación), the Physics School, and the CICANUM Research Center of the Universidad de Costa Rica, for funding the CARTA 2016-2018 Project (915-B6-156), as well as the Costa Rica National Park System (Sistema Nacional de Áreas de Conservación-SINAC and the Area de Conservación de la Cordillera Volcánica Central-ACCVC) for access to Costa Rican volcanoes. We also thank INETER, the Policia Nacional de Nicaragua, and the Instituto Nicaragüense de Aeronáutica Civil, especially José Pinell, for access and escort to Volcán Masaya. All data generated by this project are included in this paper as tables and figures.

References

Aiuppa, A., de Moor, M., Arellano, S., Coppola, D., Francofonte, V., Galle, B., et al. (2018). Tracking formation of a lava lake from ground and space: Masaya volcano (Nicaragua), 2015–2017. *Geochemistry, Geophysics, Geosystems*, *19*, 496–515. https://doi.org/10.1002/2017GC007227

Aiuppa, A., Federico, C., Giudice, G., Gurrieri, S., Liuzzo, M., Shinohara, H., et al. (2006). Rates of carbon dioxide plume degassing from Mount Etna volcano. *Journal of Geophysical Research*, *111*, B09207. https://doi.org/10.1029/2006JB004307

Aiuppa, A., Moretti, R., Federico, C., Giudice, G., Gurrieri, S., Liuzzo, M., et al. (2007). Forecasting Etna eruptions by real-time observation of volcanic gas composition. *Geology*, *35*(12), 1115–1118. https://doi.org/10.1130/G24149A.1

Andres, R. J., & Kasgnoc, A. D. (1998). A time-averaged inventory of subaerial volcanic sulfur emissions. *Journal of Geophysical Research*, *103*(D19), 25,251–25,261. https://doi.org/10.1029/98JD02091

Conde, V., Robidoux, P., Avard, G., Galle, B., Aiuppa, A., Muñoz, A., & Giudice, G. (2014). Measurements of volcanic SO_2 and CO_2 fluxes by combined DOAS, Multi-GAS and FTIR observations: A case study from Turrialba and Telica volcanoes. *International Journal of Earth Sciences*, *103*(8), 2335–2347. https://doi.org/10.1007/s00531-014-1040-7

de Moor, J. M., Aiuppa, A., Avard, G., Wehrmann, H., Dunbar, N., Muller, C., et al. (2016). Turmoil at Turrialba volcano (Costa Rica): Degassing and eruptive processes inferred from high-frequency gas monitoring. *Journal of Geophysical Research: Solid Earth*, *121*, 5761–5775. https://doi.org/10.1002/2016JB013150

de Moor, J. M., Aiuppa, A., Pacheco, J., Avard, G., Kern, C., Liuzzo, M., et al. (2016). Short-period volcanic gas precursors to phreatic eruptions: Insights from Poás Volcano, Costa Rica. *Earth and Planetary Science Letters*, *442*, 218–227. https://doi.org/10.1016/j.epsl.2016.02.056

de Moor, J. M., Kern, C., Avard, G., Muller, C., Aiuppa, A., Saballos, A., et al. (2017). A new sulfur and carbon degassing inventory for the Southern Central American Volcanic Arc: The importance of accurate time-series data sets and possible tectonic processes responsible for temporal variations in arc-scale volatile emissions. *Geochemistry, Geophysics, Geosystems*, *18*, 4437–4468. https://doi.org/10.1002/2017GC007141

Diaz, J. A., Pieri, D., Wright, K., Sorensen, P., Kline-Shoder, R., Arkin, C. R., et al. (2015). Unmanned aerial mass spectrometer systems for in-situ volcanic plume analysis. *Journal of the American Society for Mass Spectrometry*, *26*(2), 292–304. https://doi.org/10.1007/s13361-014-1058-x

Faivre-Pierret, R., Martin, D., & Sabroux, J.-C. (1980). Contribution des sondes aérologiques motorisées à l'étude de la physico-chimie des panaches volcaniques. *Bulletin Volcanologique*, *43*(3), 473–485. https://doi.org/10.1007/BF02597686

Galle, B., Oppenheimer, C., Geyer, A., McGonigle, A. J. S., Edmonds, M., & Horrocks, L. (2003). A miniaturised ultraviolet spectrometer for remote sensing of SO_2 fluxes: A new tool for volcano surveillance. *Journal of Volcanology and Geothermal Research*, *119*(1-4), 241–254. https://doi.org/10.1016/S0377-0273(02)00356-6

Gerlach, T. M., Delgado, H., McGee, K. A., Doukas, M. P., Venegas, J. J., & Cárdenas, L. (1997). Application of the LI–COR CO_2 analyzer to volcanic plumes: A case study, Volcán Popocatépetl, Mexico, June 7 and 10, 1995. *Journal of Geophysical Research*, *102*, 8005–8019. https://doi.org/10.1029/96JB03887

Giggenbach, W. F. (1975). Variations in the carbon, sulfur and chlorine contents of volcanic gas discharges from White Island, New Zealand. *Bulletin of Volcanology*, *39*, 15–1927. https://doi.org/10.1007/BF02596943

Global Volcanism Program (2017a). Report on Turrialba (Costa Rica). In S. K. Sennert (Ed.), *Weekly volcanic activity report, 3 May–9 May 2017*. Washington, DC: Smithsonian Institution and US Geological Survey.

Global Volcanism Program (2017b). Report on Masaya (Nicaragua). In E. Venzke (Ed.), *Bull. global volcanism network* (Vol. 42, p. 9). Washington, DC.

Hilton, D. R., Fischer, T. P., McGonigle, A. J. S., & de Moor, J. M. (2007). Variable SO_2 emission rates for Anatahan volcano, the Commonwealth of the Northern Mariana Islands: Implications for deriving arc-wide volatile fluxes from erupting volcanoes. *Geophysical Research Letters*, *34*, L14315. https://doi.org/10.1029/2007GL030405

Horton, K. A., Williams-Jones, G., Garbeil, H., Elias, T., Sutton, A. J., Mouginis-Mark, P., et al. (2006). Real-time measurement of volcanic SO_2 emissions: Validation of a new UV correlation spectrometer (FLYSPEC). *Bulletin of Volcanology*, *68*(4), 323–327. https://doi.org/10.1007/s00445-005-0014-9

21699356, 2018, 8, Downloaded from https://agupubs.onlinelibrary.wiley.com/doi/10.1029/2018JB015655 by Cochrane Costa Rica, Wiley Online Library on [14/11/2025]. See the Terms and Conditions (https://onlinelibrary.wiley.com/terms-and-conditions) on Wiley Online Library for rules of use; OA articles are governed by the applicable Creative Commons License

Johansson, M., & Zhang, Y. (2004). Mobile DOAS, version 4.4, Optical Remote Sensing Group, Chalmers University of Technology

Kern, C., Deutschmann, T., Vogel, L., Wöhrbach, M., Wagner, T., & Platt, U. (2009). Radiative transfer corrections for accurate spectroscopic measurements of volcanic gas emissions. *Bulletin of Volcanology*, *72*(2), 233–247. https://doi.org/10.1007/s00445-009-0313-7

Kern, C., Masias, P., Apaza, F., Reath, K. A., & Platt, U. (2017). Remote measurement of high preeruptive water vapor emissions at Sabancaya volcano by passive differential optical absorption spectroscopy. *Journal of Geophysical Research: Solid Earth*, *122*, 3540–3564. https://doi.org/10.1002/2017JB014020

Liotta, M., Rizzo, A., Paonita, A., Caracausi, A., & Martelli, M. (2012). Sulfur isotopic compositions of fumarolic and plume gases at Mount Etna (Italy) and inferences on their magmatic source. *Geochemistry, Geophysics, Geosystems*, *13*, Q05015. https://doi.org/10.1029/2012GC004118

Martin, R. S., Sawyer, G. M., Day, J. A., LeBlond, J. S., Ilyinskaya, E., & Oppenheimer, C. (2012). High-resolution size distributions and emission fluxes of trace elements from Masaya volcano, Nicaragua. *Journal of Geophysical Research*, *117*, B08206. https://doi.org/10.1029/2012JB009487

Mather, T. A., Pyle, D. M., Tsanev, V. I., McGonigle, A. J. S., Oppenheimer, C., & Allen, A. G. (2006). A reassessment of current volcanic emissions from the Central American arc with specific examples from Nicaragua. *Journal of Volcanology and Geothermal Research*, *149*(3-4), 297–311. https://doi.org/10.1016/j.jvolgeores.2005.07.021

McGonigle, A. J. S., Aiuppa, A., Giudice, G., Tamburello, G., Hodson, A. J., & Gurrieri, S. (2008). Unmanned aerial vehicle measurements of volcanic carbon dioxide fluxes. *Geophysical Research Letters*, *35*, L06303. https://doi.org/10.1029/2007GL032508

Mori, T., Hashimoto, T., Terada, A., Yoshimoto, M., Kazahaya, R., Shinohara, H., & Tanaka, R. (2016). Volcanic plume measurements using a UAV for the 2014 Mt. Ontake eruption. *Earth, Planets and Space*, *68*(1), 1861. https://doi.org/10.1186/s40623-016-0418-0

Moune, S., Gauthier, P.-J., & Delmelle, P. (2010). Trace elements in the particulate phase of the plume of Masaya volcano, Nicaragua. *Journal of Volcanology and Geothermal Research*, *193*(3-4), 232–244. https://doi.org/10.1016/j.jvolgeores2010.04.004

Nadeau, P. A., & Williams-Jones, G. (2009). Apparent downwind depletion of volcanic SO_2 flux - lessons from Masaya volcano, Nicaragua. *Bulletin of Volcanology*, *71*(4), 389–400. https://doi.org/10.1007/s00445-008-0251-9

Rüdiger, J., Tirpitz, J.-L., de Moor, J. M., Bobrowski, N., Gutmann, A., Liuzzo, M., et al. (2018). Implementation of electrochemical, optical and denuder-based sensors and sampling techniques on UAV for volcanic gas measurements: Examples from Masaya, Turrialba and Stromboli volcanoes. *Atmospheric Measurement Techniques*, *11*(4), 2441–2457. https://doi.org/10.5194/amt-11-2441-2018

Rymer, H., van Wyk de Vries, B., Stix, J., & Williams-Jones, G. (1998). Pit crater structure and processes governing persistent activity at Masaya volcano, Nicaragua. *Bulletin of Volcanology*, *59*(5), 345–355. https://doi.org/10.1007/s004450050196

Shinohara, H. (2005). A new technique to estimate volcanic gas composition: Plume measurements with a portable multi-sensor system. *Journal of Volcanology and Geothermal Research*, *143*(4), 319–333. https://doi.org/10.1016/j.jvolgeores.2004.12.004

Shinohara, H. (2013). Composition of volcanic gases emitted during repeating Vulcanian eruption stage of Shinmoedake, Kirishima volcano, Japan. *Earth Planets Space*, *65*, 667–675. https://doi.org/10.5047/eps.2012.11.001

Shinohara, H., Kazahaya, K., Saito, G., Fukui, K., & Odai, M. (2003). Variation of CO_2/SO_2 ratio in volcanic plumes of Miyakejima: Stable degassing deduced from heliborne measurements. *Geophysical Research Letters*, *30*(23), 1208. https://doi.org/10.1029/2002GL016105

Stoiber, R. E., & Williams, S. N. (1986). Sulfur and halogen gases at Masaya caldera complex, Nicaragua—Total flux and variations with time. *Journal of Geophysical Research*, *91*(B12), 12,215–12,231. https://doi.org/10.1029/JB091iB12p12215

Werner, C., Hurst, T., Scott, B., Sherburn, S., Christenson, B. W., Britten, K., et al. (2008). Variability of passive gas emissions, seismicity, and deformation during crater lake growth at White Island volcano, New Zealand, 2002-2006. *Journal of Geophysical Research*, *113*, B01204. https://doi.org/10.1029/2007JB005094

Williams-Jones, G., Horton, K. A., Elias, T., Garbeil, H., Mouginis-Mark, P. J., Sutton, A. J., & Harris, A. J. (2006). Accurately measuring volcanic plume velocity with multiple UV spectrometers. *Bulletin of Volcanology*, *68*(4), 328–332. https://doi.org/10.1007/s00445-005-0013-x

Wittmer, J., Bobrowski, N., Liotta, M., Giuffrida, G., Calabrese, S., & Platt, U. (2014). Active alkaline traps to determine acidic-gas ratios in volcanic plumes: Sampling techniques and analytical methods. *Geochemistry, Geophysics, Geosystems*, *15*, 2797–2820. https://doi.org/10.1002/2013GC005133

Xi, X., Johnson, M. S., Jeong, S., Fladeland, M., Pieri, D., Diaz, J. A., et al. (2016). Constraining the sulfur dioxide degassing flux from Turrialba volcano, Costa Rica using unmanned aerial system measurements. *Journal of Volcanology and Geothermal Research*, *325*, 110–118. https://doi.org/10.1016/j.jvolgeores.2016.06.023

Zelenski, M. E., Fischer, T. P., de Moor, J. M., Marty, B., Zimmermann, L., Ayalew, D., et al. (2013). Trace elements in the gas emissions from the Erta Ale volcano, afar, Ethiopia. *Chemical Geology*, *357*, 95–116. https://doi.org/10.1016/j.chemgeo2013.08.022

21699356, 2018, 8, Downloaded from https://agupubs.onlinelibrary.wiley.com/doi/10.1029/2018JB015655 by Cochrane Costa Rica, Wiley Online Library on [14/11/2025]. See the Terms and Conditions (https://onlinelibrary.wiley.com/terms-and-conditions) on Wiley Online Library for rules of use; OA articles are governed by the applicable Creative Commons License